DELIVERABLE 5.3.3

Advancement in application of advanced oxidation methods for cleaning of decontamination waste waters

Dissemination level: **public**

WP5

Decontamination procedures of water distribution systems

1. August, 2012

Project n°217976

Contact persons
Sylvain FASS sylvain.fass@univ-lorraine.fr
Jean Claude BLOCK
jean-claude.block@ univ-lorraine.fr

List of Deliverable 5.3.3 contributors:

From RTU

Janis Rubulis (janis.rubulis@gmail.com)

Kamila Gruskevica (kamila.gruskevica@rtu.lv)

Talis Juhna (talis.juhna@rtu.lv)

Kristina Tihomirova

Sandis Dejus

Janis Neilands

Janis Sprogis

From FEUP

Luis Miguel Madeira

Cátia Oliveira

Arminda Alves

Abstract

Water resources and systems are attractive targets for terrorists' attacks because there is no substitute for water. Contamination agents such as pesticides and spores can be easily spread via water supply systems and affect large number of population. Even at low doses pesticides and *Bacillus anthracis* spores are dangerous for humans. Conventional decontamination methods include usage of strong oxidants which may not always effective especially for removal contaminates which are accumulated on the surfaces of the pipes, moreover, they may also be highly reactive and thus forming complexes with organic material and promoting distribution system corrosion. Thus decontamination approach providing as less treatment by-products as possible is needed. The Fenton's reagent is a technology, widely used in wastewater treatment and is safe (no hazardous residues are produced). Therefore, in this study (task 5.5) the Secureau team aimed to test:

- **use of pipe deposits from water networks as novel catalysts in paraquat peroxidation** - FEUP (partner 7). In the event of a network contamination, the deposits present in the pipes (that often contain considerable amounts of iron) can be directly used to catalyse the process *in situ*, without requiring the insertion of chemicals (apart from the oxidant – H_2O_2). Four real pipe deposits with different chemical compositions and morphological properties were tested as catalysts in paraquat heterogeneous peroxidation. Results showed that some of the deposits taken from water networks can be used as catalysts in the peroxidation of paraquat. The deposits are quite complex and the reasons for their completely different performances are not yet completely clear. Probably the form of iron oxides presented in deposits and also presence of other metals and substances plays important role. A better degradation is achieved when water was acidified to the pH of 3.0. Depending on the types of solids present in the network, in situ treatment can be made without insertion of chemicals apart from the oxidant, in case of a contamination event.

- **efficacy of Fenton reaction for removal of paraquat pesticide in a pilot plant** FEUP (partner 7) and RTU (oartner 8). Fenton-like reaction was tested for the elimination of paraquat in water in a pilot loop. The treatment method which showed best results for paraquat decomposition from previous parametric study in a stirred batch reactor (deliverable 5.3.1) was used. In current study loose deposits, instead of ferrous iron, were performed to evaluate an ability of solid to catalyze the process. Also the ability of distribution system pipes to catalyze reaction was tested. The results show that paraquat degradation can be done in the pilot loop, achieving similar results to those obtained in lab scale reactor. Loose deposits can be used as catalysts, but special care must be taken to their composition, as well as the amount used / present in water pipes. Cast iron pipes also have positive effect on the oxidation process. Bigger percentage of cast iron pipes in the experiments resulted in the bigger contribution in the heterogeneous process, but special attention is required to measure the decrease in the thickness of those pipes for long term use, once they can be solubilized. The gradual addition of hydrogen peroxide showed to

be the best option in the oxidation process, allowing reaching higher mineralization degrees.

- **Using of Fenton reaction for inactivation of *B. subtilis* spores in water** RTU - (partner 8). In this section Fenton reaction was used to inactivate *B. subtilis* spores in water. Copper and iron were tested as catalysts for Fenton reaction. Treatment approach used by FEUP for decomposition of paraquat did not show significant reduction in concentration of viable spores of *B. subtilis*. None of the tested approaches using Fe as a catalyst resulted in visible spore reduction. The results showed that it is possible to inactivate *B.subtilis* spores rapidly and effectively in water using copper as a transition metal and ascorbic acid as a catalyst can be achieved without pH correction.

Content

1 Use of pipe deposits from water networks as novel catalysts in paraquat peroxidation

1.1 Introduction

Contamination of water courses with chemical compounds, namely pesticides, is an increasing concern due to their toxicity. Among pesticides, paraquat (PQ) is one of the most hazardous, being also of concern its high solubility in water (620 g/L). Its use in agriculture as a pesticide and its high mobility in the soils have led to increasing levels of this compound in ground water. Even at very low doses, this herbicide can pass some treatment steps in a water treatment plant and reach the drinking water of the water distribution systems (Klamerth *et al.*, 2010). For these reasons, paraquat represents a threat to human health. Beyond the natural occurrence of paraquat in water due to its large usage in some countries, it could be found in this matrix by other ways. The main objective of the SecurEau project is to detect anomalous situations and treat the water of distribution systems in case of a deliberate contamination event. Accordingly, in those circumstances, the paraquat concentration in water could be very high, fact that is possible due to its high solubility in water.

Thus, the peroxidation (or Fenton) process was proposed to degrade paraquat. The Fenton's reagent is a non-expensive technology, widely used in wastewater treatment. The process involves a complex mechanism in which the parent molecules are oxidized into other organic compounds and ultimately into carbon dioxide and water (Eqs. 1 – 2). According to several authors (Walling, 1975; Pérez *et al.*, 2002), the organic matter oxidation is promoted by the hydroxyl radicals formed in the reaction between hydrogen peroxide and iron (II) (Eq.3). The catalyst, Fe (II), is restored by the reaction of hydrogen peroxide with Fe^{3+} (Fenton-like process) (Eqs. 4 – 5).

$$Organic\ \ matter + HO^{\cdot} \rightarrow Oxidation\ \ intermediates \quad (1)$$

$$Oxidation\ \ intermediates + HO^{\cdot} \rightarrow CO_2 + H_2O \quad (2)$$

$$Fe^{2+} + H_2O_2 \rightarrow Fe^{3+} + OH^{-} + HO^{\cdot} \quad (3)$$

$$Fe^{3+} + H_2O_2 \rightarrow FeOOH^{2+} + H^{+} \quad (4)$$

$$FeOOH^{2+} \rightarrow HO_2^{\cdot} + Fe^{2+} \quad (5)$$

In order to reduce the amounts of reagents used in the process (namely ferrous solutions), and trying to avoid the formation of iron sludge, the possibility of using iron-containing materials, or solids with iron attached to its surface, has been widely addressed by several authors through the so-called heterogeneous Fenton-like (or photo-Fenton-like) processes (Herney-Ramirez *et al.*, 2010; Duarte *et al.*, 2009; Navalon *et al.*, 2010). In most cases these materials are used to support the iron species, being worth of mentioning the use of clays (Navalon *et al.*, 2010; Garrido-Ramirez *et al.*, 2010; Feng *et al.*, 2003; Ramirez *et al.*, 2007; Hassan and Hameed, 2011), activated carbons (Fontecha-Cámara *et al.*, 2011; Duarte *et al.*, 2011; Nguyen *et al.*, 2011), or zeolites (Navalon *et al.*, 2010; Duarte and Madeira, 2010; Kusić *et al.*, 2006; Tekbas *et al.*, 2008; Dükkanci *et al.*, 2010). Besides, catalyst separation and recovery is also promoted with this approach.

Deposits that exist in water networks are mainly of two types: loosely or firmly attached. They are thus often discarded, either after networks cleaning (loosely deposits), or during maintenance operations (when firmly attached). In the event of a network contamination, the deposits present in the pipes (that often contain considerable amounts of iron) can be directly used to catalyse the process *in situ*, without requiring the insertion of chemicals (apart from the oxidant – H_2O_2).

Four real pipe deposits with different chemical compositions and morphological properties were characterized and tested as catalysts in paraquat heterogeneous peroxidation, aiming trying to correlate solid's properties/composition with their catalytic performance. For the deposit with better performance a study of the pH effect was made, because this is a variable of paramount importance in the designed applications; particular emphasis was given for exploring the possibility of operating in non-acidic conditions that are commonly optimal for Fenton's oxidation.

1.2 Materials and methods

1.2.1 Reagents

Paraquat dichloride (PQ) PESTANAL® analytical standard, 99.2% (from Fluka), was purchased from Sigma Aldrich (St. Louis, USA). Hydrogen peroxide solution (30% v/v), iron (II) sulphate heptahydrate (99.5%) and anhydrous sodium sulphite were purchased from Merck (Darmstadt, Germany). Sulphuric acid (96%) was from José M. Vaz Pereira, Lda (Lisbon, Portugal), while sodium hydroxide (98.7%) was from José Manuel Gomes dos Santos, Lda (Odivelas, Portugal). Heptafluorobutyric acid (HFBA) was from Sigma Aldrich, and acetonitrile (HPLC grade) from Prolabo.

1.2.2 Standards preparation

Experiments were conducted with paraquat solutions of 100 mg/L, which were prepared diluting the appropriate amount of paraquat analytical standard in distilled water. All paraquat solutions were stored at 4 ºC in polypropylene containers, in which adsorption does not occur. These solutions are stable when exposed to the used conditions (room temperature and while stored at 4 ºC or frozen).

1.2.3 Deposits treatment and characterization

The samples used as catalysts in the oxidation studies were taken from real drinking water distribution systems. The deposits were removed from old cast iron pipes that needed to be substituted. It is known that temperature can produce structural changes in these solids. As a way to avoid it, preliminary tests were done to find out which type of drying should be used with these materials. Deposits were submitted to drying in an oven (till no weight variation has been detected), at 100, 150 and 200 ºC. Then, all deposits were sieved and sorted by particle size, according to the ranges: i) $d_p < 38$ µm, ii) $38 < d_p < 63$ µm, iii) $63 < d_p < 150$ µm, iv) $150 < d_p < 300$ µm and v) $300 < d_p < 500$ µm. The different fraction sizes were kept in dry conditions until the experiments.

Inductively coupled plasma optical emission spectrometry (ICP-OES) has been used for quantitative analysis of the elemental composition of the deposits. In detail, a Vista Pro ICP-OES (Varian) apparatus, equipped with a SPS3 autosampler (Varian) was used. Samples were prepared by microwave digestion of the deposits in *aqua regia*.

The BET surface area of the solids was determined by N_2 adsorption at 77 K in a Quantachrome Autosorb-1

apparatus, while X-ray diffraction (XRD) was carried out with a Bruker D8 Advance diffractometer using Cu Kα radiation. Identification of the crystallographic phases present was based on the files from JCPDS (Joint Committee on Powder Diffraction Standards).

The morphology of the deposits was analysed in a JEOL JSM 6301F scanning electron microscope (SEM) equipped with an EDS micro-analysis system (Oxford INCA Energy 350). During micro-analyses an accelerating voltage of 15kV was used. The samples for SEM analyses were dispersed on a carbon tape and then coated with a thin film of Au – Pd alloy (about 20 nm) to achieve the necessary surface conductivity.

The pH_{pzc} (point of zero charge) of the solids was determined according to the procedure reported by Rivera-Utrilla *et al.*(2001), which consists in the use of several flasks with 50 mL of 0.01 M NaCl, adjusting the pH to values in the range of 2 to 12, with 0.01 M HCl or 0.01 M NaOH. Into each flask was added 0.30 g of sample and stirring proceeded for 48 h, at room temperature. After this period, the pH was measured. The interception of the plot pH_{final} *vs*. $pH_{initial}$ with the plot $pH_{final} = pH_{initial}$ gives the value of pH_{pzc} (Rivera-Utrilla *et al.*, 2001).

1.2.4 Analytical methods

The paraquat degradation was followed by high performance liquid chromatography with diode array detection (HPLC-DAD). The HPLC-DAD consists in a L-2130 pump, a L-2200 auto-sampler and a L-2455 diode array detector (DAD). The chromatographic separation was achieved by a Chromolith® Performance RP-18e 100-3 column supplied by VWR, using a mobile phase with 95% (v/v) of 10 mM HFBA in water and 5% (v/v) of acetonitrile, at isocratic conditions, with a flow rate of 1 mL min^{-1}. Injection volume was 99 µL. The spectra acquisition was done from 220 to 400 nm and paraquat was quantified at 259 nm, with a retention time of ca. 3 min. This method is characterized by a detection limit of 0.03 mg/L and a quantification limit of 0.08 mg/L.

The samples collected along the reactions were also analysed in a TC/TOC analyser (Shimadzu 5000A) to evaluate the mineralization degree. The total organic carbon (TOC) present in each sample was calculated by subtracting the inorganic carbon from the total carbon (TC), both determined following the standard method 5310 D in the American Public Health Association (APHA, 1998). For this methodology, a calibration curve was obtained up to 100 mg/L; detection limits of 0.27 mg/L and 0.63 mg/L were attained for total carbon and inorganic carbon, respectively. TOC values reported represent the average of at least two measurements; in most cases each sample was injected three times, validation being performed by the apparatus only if the CV (coefficient of variation) is smaller than 2%.

The metals in the solution were determined using a UNICAM 939/959 flame atomic absorption spectrophotometer.

1.2.5 Oxidation experiments

Oxidation reactions were carried out in a slurry stirred batch reactor with 250 mL of capacity. The temperature and the pH of the reaction mixture were respectively measured by a thermocouple and a pH electrode (WTW, SenTix 41 model), connected to a pH-meter from WTW (model Inolab pH Level 2). The temperature was kept constant in the desired value by a Huber thermostatic bath (Polystat CC1 unit) that ensured water recirculation through the jacket of the reactor. No temperature variations higher than ± 1 ºC were observed. After temperature stabilisation, the pH of the PQ solution was adjusted to the desired value by adding small amounts of 2 M H_2SO_4 or NaOH aqueous solutions. The start of the oxidation process was remarked by the addition of the catalyst (solid deposit or iron salt, the later for homogenous experiments) and the oxidant agent (hydrogen peroxide). In some cases, described in the text, pH was re-adjusted after solid addition, but the initial instant of reaction coincided again with the H_2O_2 insertion into the reactor. During the reaction, samples (10 mL each)

were withdrawn, filtered with a PTFE syringe filter, and analysed as described in section 1.2.4. To stop the homogenous reaction in the vial samples an excess of Na_2SO_3 was used to instantaneously consume the remaining hydrogen peroxide.

1.3 Results and discussion

1.3.1 Deposits characterization

The elemental composition of each real deposit sample tested, herein called P12, APP1, P45 and BayCa, was obtained by the ICP-OES technique; results obtained are presented in **Erreur ! Source du renvoi introuvable.**. Iron mass percentage was 47.1%, 40.8%, 63.7% and 0.29% for P12, APP1, P45 and BayCa, respectively (dry basis). As it can be seen, the deposits P12, APP1 and P45 have a high content in aluminium, calcium, copper, silicon and particularly in iron; on the other hand, the deposit BayCa is highly rich in calcium (35.2 wt.%), with relevant contents of magnesium and sodium. All the deposits are quite complex, with numerous elements in their composition.

The BET surface areas were determined by nitrogen adsorption at 77 K, and the results obtained are shown in Table 1. The BET areas obtained for each deposit are very small, typical of non-porous materials. Only in the case of P45 sample the existence of some porosity is noticed. In Table 1 are also reported the pH_{pzc} values for all the solids, which range from 2.85 up to 8.60. This issue will have a significant impact in the catalytic performance of the materials when added into a paraquat solution, as described below.

Table 1 Composition of the inorganic deposit samples used (determined by ICP-OES) and corresponding BET areas (determined by N_2 adsorption) and pHpzc values

Element	Samples Composition (mg/kg of deposit, dry basis)			
	P12	APP1	P45	BayCa
Al	1610	1240	882	413
Ca	3860	3010	996	352000
Cd	46.0	1.8	13.5	0.2
Co	27.7	32	27.0	1.9
Cr	15.7	13.2	75.2	1.0
Cu	1130	986	145	72.8
Fe	471000	408000	637000	2910
K	<790	<400	<600	<300
Mg	<790	322	<600	2990
Mn	126	123	4390	894
Na	<790	<400	<600	1060
Ni	42.3	39.9	183	6.3
Pb	33.4	8.8	40.3	2.4
P	315	345	7830	102
Si	2600	1090	1970	819
Zn	92.2	74	2630	47.6
Water content, wt. %	29.2	35.4	30.0	11.4
S_{BET}, m^2/g	7	5	36	1
pH_{pzc}	2.85	3.33	5.99	8.60

The deposits were also analysed by x-ray diffraction. The diffraction patterns are presented in

Figure 1, together with the identification of the most relevant iron oxides present in each sample. Due to the complex nature of all the solids, it would be quite difficult to identify all the species present in each of them. Therefore, the search was mainly focused on iron-based oxides, because iron is the most active metal for Fenton-like processes and in the majority of the solids it is the predominant metal; however, there are many different allotropic forms of iron oxides-hydroxides, which can be transformed easily between them. The broad and low intensity peaks point out the low crystallinity of the residues P12, APP1 and P45. These deposits are basically a mixture of iron oxyhydroxides, in the case of P12 corresponding to the ferroxyhyte, δ-FeO(OH) (file 13-518). Additionally, akaganéite (file 42-1315), the Fe^{3+}oxide-hidroxide/chloride ($Fe^{3+}O(OH,Cl)$) that can be formed by the chlorine used in drinking water networks, can be identified by peaks at 27.0 and 35.3 º. Peaks at 26.4 and 50.1 º are indicative of the presence of quartz and the multiple peaks in the region between 25-30º can mask also the presence of compounds such as bassanite ($CaSO_4 \cdot H_2O$, file 14-453) or feldspat (Kaolinite, muscovite, etc). The XRD peaks of deposit APP1 correspond to lepidocrocite, γ-FeO(OH) (file 8-98), and goethite, α-FeO(OH), or $Fe_2O_3 \cdot H_2O$ (file 17-536). In the deposit P45 goethite can be also easily identified. The most pure and crystalline sample is the deposit BayCa and, for that reason, the easiest to identify the existing components. The peaks clearly match calcite, i.e., calcium carbonate – $CaCO_3$ (file 5-586).

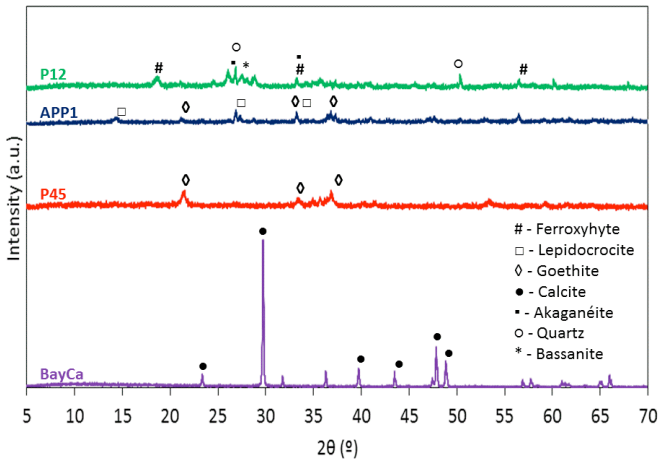

Figure 1: XRD patterns obtained for all the deposits.

The deposits were also analysed by SEM – Scanning Electron Microscopy. Microphotographs of each deposit are shown in Figure 2. As it can be seen, the deposits used have different morphologies: deposit P12 has a laminar morphology and some clusters of smaller particles; deposit APP1 has a blend of particles with a laminar morphology and particles with a spherical shape; deposit P45 is characterized by particles with an imperfect shape, looking like clusters of smaller particles; deposit BayCa possesses particles with perfect laminar faces.

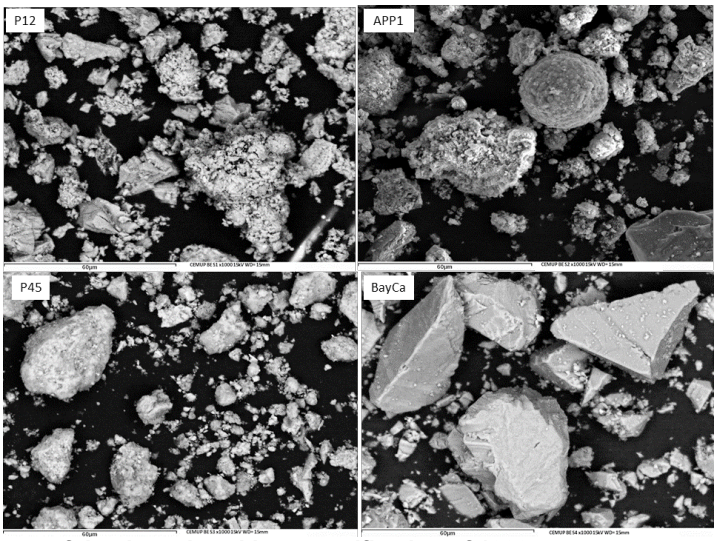

Figure 2: SEM pictures of the deposits with a magnification of 1000x.

According to Echeverría *et al*. (2009), deposits from a water distribution system can be classified in three different categories, according to their composition: brown deposits, tubercle deposits and white deposits. Brown deposits are composed by aluminosilicates, humic acids and quartz. Tubercles are mainly comprised by magnetite and goethite and in some cases lepidocrocite. White deposits are essentially composed by calcite, aluminosilicates and quartz. From this information, the identification of each deposit used can be done: deposits P12 and APP1 can be included in the group of brown deposits, whereas P45 can be identified as a tubercle deposit, and BayCa is clearly a white deposit. So, deposits used in this project are typical and representative of those found in water distribution systems.

1.3.2 Paraquat Oxidation

According to a parametric study previously done to evaluate the influence of some parameters in the paraquat degradation by the homogeneous Fenton's process (cf. deliverable 5.5), the conditions that led to a good compromise between high mineralization degree and low reagents consumption were the following: T = 30 ºC, pH_0 = 3, $[H_2O_2]_0 = 1.5 \times 10^{-2}$ M and $[Fe(II)] = 5.0 \times 10^{-4}$ M, for $[PQ]_0 = 3.98 \times 10^{-4}$ M. For that reason, the study with pipe deposits was initiated using the double of the initial iron concentration and keeping constant the other parameters. A double amount in the iron concentration was used because, with the inorganic deposits, the iron is not so available, being expected to be needed higher quantities of catalyst to reach the same results (if attainable); besides, the iron species are not so active (different oxidation state, etc.).

1.3.3 Preliminary assays

First of all, some preliminary experiments were performed. With such experiments it was possible to conclude that:

- No degradation of paraquat pesticide was noticed in the presence of hydrogen peroxide alone. Although H_2O_2 is a well-known oxidizing agent, its oxidation potential is much lower than that of the hydroxyl radicals (Bigda, 1995), which formation requires the presence of the iron catalyst.
- The hydrogen peroxide concentration effect in the paraquat degradation was assessed. Concentrations of 1.5×10^{-2} M, 3.0×10^{-2} M and 7.5×10^{-3} M were tested, but the best performance was found for the peroxide concentration of 1.5×10^{-2} M (the same as in the homogenous process, thus evidencing the existence of an optimum oxidant dose, which is typical in peroxidation processes - cf. deliverable 5.5).
- No adsorption of the pesticide occurs for the employed conditions and with the pipe deposits used.
- In the range of temperatures selected for drying the samples in the oven (100 – 200 ºC), no effect was noticed in their catalytic performances. This allows concluding that the solids are completely dried and no important phase changes occurred.
- The wet deposits were also tested, and it was found that if the water content is taken into account in the mass of weighted catalyst putted into the reactor, they can be used with no previous drying or any other treatment.
- Some experiments were repeated and very good reproducibility was found (deviation < 5 %).
- For all the deposits it was observed that the particle size has almost no effect in the paraquat degradation and mineralization (the differences are smaller than 5-10 %), whereby it was decided to blend all particle sizes and work with the resultant mixture. The fact that no effect of the particle size was noticed can be attributed to the absence of internal mass transfer resistances. This, in turn, is related with the absence of significant internal porosity, as evidenced by the very low surface areas of these materials (**Erreur ! Source du renvoi introuvable.**).

1.3.4 Study of the deposits catalytic performance

In this section, it was compared the paraquat degradation and mineralization performance for each inorganic deposit (taking into account the iron content in each one, given in **Erreur ! Source du renvoi introuvable.**, i.e., adjusting the mass of catalyst so that the total iron load is the same – 1.0×10^{-3} M). These assays were performed adjusting the pH of the paraquat solution only before the solid addition (and without any further pH re-adjustment). Figure 3 indicates that deposits P45 and BayCa did not lead to a good pesticide degradation (actually with sample P45 no decline in PQ concentration was noticed) in opposition to deposits P12 and APP1. Additionally, deposit P12 presents the best degradation degree, being possible to completely eliminate PQ after ca. 2.5 h of

reaction. With this sample, a TOC reduction above 40 % was obtained after 6 h (Figure 4).

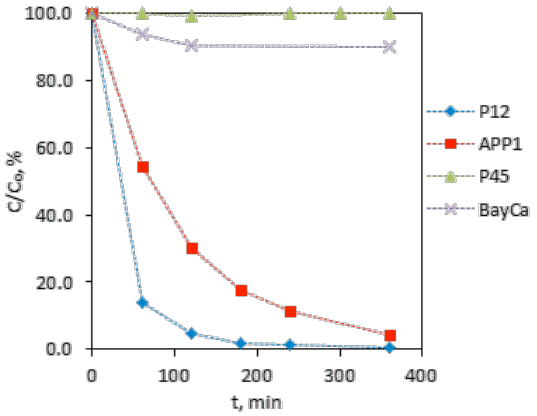

Figure 3: Paraquat degradation along the reaction using the different deposits ([P12] = 118.6 mg/L, [APP1] = 136.8 mg/L, [P45] = 87.6 mg/L, [BayCa] = 19192 mg/L) without pH re-adjustment after solid addition (T = 30 ºC, pH_0 = 3, $[PQ]_0 = 3.98 \times 10^{-4}$ M, $[H_2O_2]_0 = 1.5 \times 10^{-2}$ M and [Fe] = 1.0×10^{-3} M).

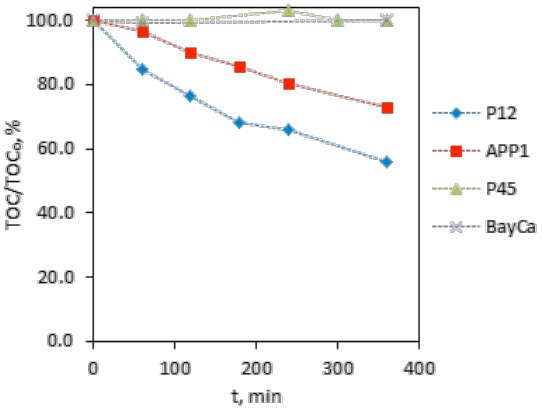

Figure 4: Paraquat mineralization along the reaction using the different deposits ([P12] = 118.6 mg/L, [APP1] = 136.8 mg/L, [P45] = 87.6 mg/L, [BayCa] = 19192 mg/L) without pH re-adjustment after solid addition (T = 30 ºC, pH_0 = 3, $[PQ]_0 = 3.98 \times 10^{-4}$ M, $[H_2O_2]_0 = 1.5 \times 10^{-2}$ M and [Fe] = 1.0×10^{-3} M).

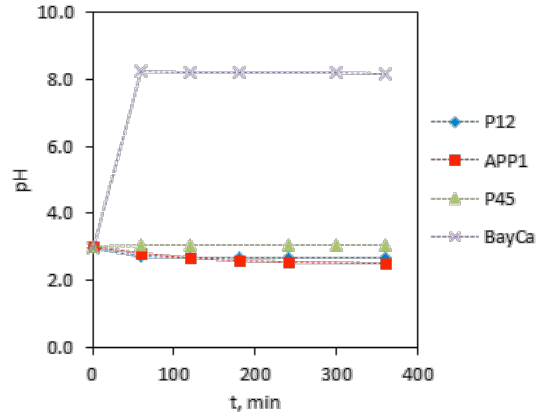

Figure 5: Evolution of the pH along the reaction using the different deposits ([P12] = 118.6 mg/L, [APP1] = 136.8 mg/L, [P45] = 87.6 mg/L, [BayCa] = 19192 mg/L) without pH re-adjustment after solid addition (T = 30 ºC, pH_0 = 3, $[PQ]_0 = 3.98 \times 10^{-4}$ M, $[H_2O_2]_0 = 1.5 \times 10^{-2}$ M and [Fe] = 1.0×10^{-3} M).

To better clarify the reasons why deposits P45 and BayCa do not work as catalysts, some issues should be highlighted. First, one should remark that according to the XRD analyses, the presence

of calcite in deposit BayCa was detected, and inherently of carbonate/bicarbonate ions in solution, which are known for their scavenger activity towards hydroxyl radicals, as it can be seen in Eqs. 7 – 8 (Lu *et al.*, 1997). This explains the very low activity of such material. Besides, a strong increase of the pH along the reaction was observed (Figure 5), also related to the high pH_{pzc} of this deposit – **Erreur ! Source du renvoi introuvable.**. The pH along oxidation increases to values around 8, which inhibits the action of the hydroxyl radicals, due to their scavenging by the hydroxide ions in excess (Rodrigues *et al.*, 2009; Ramirez *et al.*, 2009). In addition, hydrogen peroxide stability also decreases with the pH. For deposits P12 and APP1 a slight decrease of the pH was observed along the oxidation (Figure 5), suggesting the formation of carboxylic acids as reaction products/intermediates.

$$HCO_3^- + HO^{\cdot} \rightarrow CO_3^{-\cdot} + H_2O \quad (7)$$

$$CO_3^{2-} + HO^{\cdot} \rightarrow CO_3^{-\cdot} + HO^- \quad (8)$$

Deposit P45 has a very high iron content (**Erreur ! Source du renvoi introuvable.**), which is not corroborated by its catalytic performance. In fact, as above mentioned, it has no activity at all. This solid is composed by goethite, and according to Matta *et al.* (2007), goethite has a very low catalytic activity in Fenton-like processes compared to other minerals, what can be responsible for the inactivity of this deposit. We should highlight that an experiment carried out with goethite revealed in fact a very low activity in this process and no PQ mineralization at all. On the other hand, sample P45 is the solid with the highest content of Mn (**Erreur ! Source du renvoi introuvable.**), a metal that is well-known to decompose hydrogen peroxide, not yielding the radicals (Wekesa and Ni, 2003; Wekesa *et al.*, 2011).

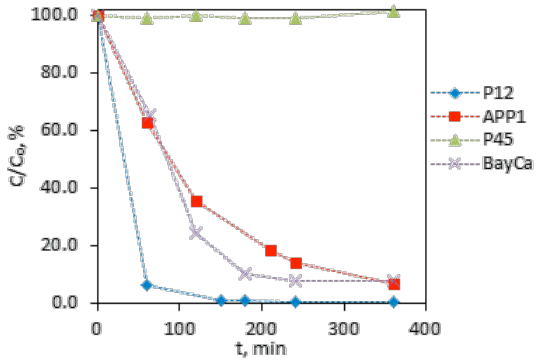

Figure 6: Paraquat degradation using the different deposits ([P12] = 118.6 mg/L, [APP1] = 136.8 mg/L, [P45] = 87.6 mg/L, [BayCa] = 19192 mg/L) with pH re-adjustment after deposit addition (T = 30 ºC, pH_0 = 3, $[PQ]_0 = 3.98 \times 10^{-4}$ M, $[H_2O_2]_0 = 1.5 \times 10^{-2}$ M and [Fe] = 1.0×10^{-3} M).

For the reasons mentioned above, further tests were performed re-adjusting the pH after the addition of the deposit to the reaction medium. Only after that, H_2O_2 was added. According to Figure 6 and Figure 7, deposit P45 still has no catalytic activity in spite of the medium pH has been re-adjusted to 3, as shown in Figure 8. On the other hand, deposit BayCa shows now a good catalytic behaviour when the pH is re-adjusted. It is important to mention that while the pH was re-adjusted, for the case of the deposit BayCa it was observed the formation of small bubbles, which

suggests the carbonates present reacted with the acid, releasing carbon dioxide. So, it was confirmed that BayCa can be employed as a catalyst, as long as the pH of the medium is kept in acidic conditions (appropriate for the Fenton's process). This proceeds through formation of hydroxyl radicals and their attack to the organic compounds (Eqs. 1 – 5). In fact, an experiment using BayCa as catalyst in the presence of a well known radical scavenger (methanol) showed that the performance is clearly affected (only 2.5 % of paraquat was degraded after 6 h).

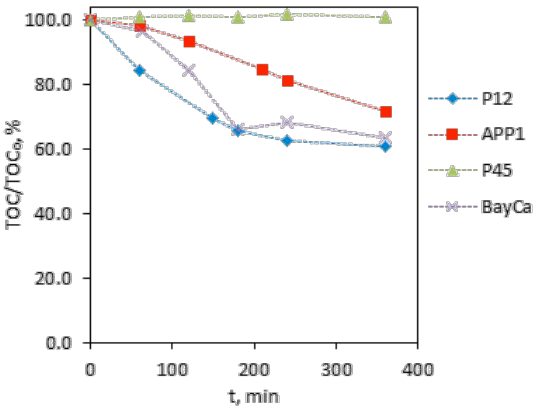

Figure 7: Paraquat mineralization using the different deposits ([P12] = 118.6 mg/L, [APP1] = 136.8 mg/L, [P45] = 87.6 mg/L, [BayCa] = 19192 mg/L) with pH re-adjustment after deposit addition (T = 30 ºC, pH_0 = 3, $[PQ]_0 = 3.98 \times 10^{-4}$ M, $[H_2O_2]_0 = 1.5 \times 10^{-2}$ M and [Fe] = 1.0×10^{-3} M).

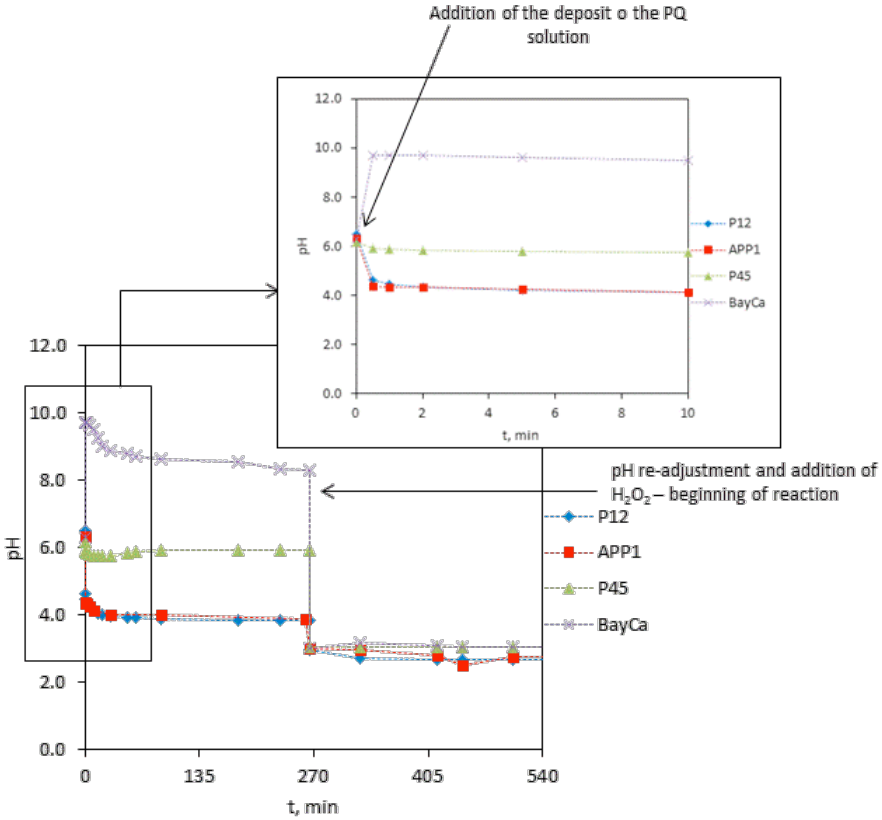

Figure 8: Evolution of the pH along the reaction using the different deposits ([P12=S1] = 118.6 mg/L, [APP1=S2] = 136.8 mg/L, [P45=S3] = 87.6 mg/L, [BayCa=S4] = 19192 mg/L) with pH re-adjustment after deposit addition (T = 30 ºC, pH_0 = 3, $[PQ]_0 = 3.98 \times 10^{-4}$ M, $[H_2O_2]_0 = 1.5 \times 10^{-2}$ M and [Fe] = 1.0×10^{-3} M).

Figure 8 shows the pH evolution of each deposit in paraquat solution (which are in line with their pH_{pzc} values – Table 4.1), and once it stabilized, the pH was adjusted to the value of 3, followed by the addition of the hydrogen peroxide to start the reaction (t = 270 min). As it can be seen, the behaviour of P12 and APP1 are similar, as well as their performance as catalysts (Figure 6 and Figure 7).

1.3.5 Study of the initial pH effect on the paraquat degradation

To study the effect of the initial pH in the degradation behaviour, the deposit with the best performance was chosen (P12). The study was performed for a pH range from 3 to 7, with the purpose of assessing the possibility of using this material in typical water pH values, not only in the acidic conditions that favour the Fenton's process.

According to the results presented in Figure 9 and Figure 10, wherein no pH re-adjustment was performed, the best performance is achieved when an initial pH of 3.0 is used. This is typical in the Fenton's chemistry (Ramirez *et al.*, 2009) and among many other issues, it can be remarked that increasing the initial pH for values higher than 3.0, the stability of the hydrogen peroxide decreases. On the other hand, if the homogeneous contribution exists, it would be smaller at higher pHs, because the metals leaching from the deposit decreases under such conditions. Besides, such iron in solution should convert into non-soluble $Fe(OH)_3$. Even so, it is remarkable that the solid still catalyses the process at initial pH values of 5 or even 7. As mentioned below, this could in part be due to the pH decrease after solid addition to the reaction medium.

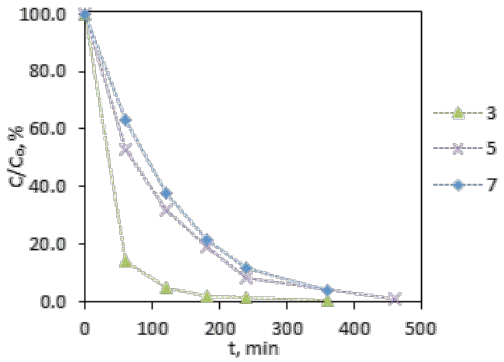

Figure 9: Effect of the initial pH on the paraquat degradation using deposit P12 (with no pH re-adjustment after deposit addition) (T = 30 ºC, $[PQ]_0 = 3.98 \times 10^{-4}$ M, $[H_2O_2]_0 = 1.5 \times 10^{-2}$ M, [P12] = 118.6 mg/L and [Fe] = 1.0×10^{-3} M).

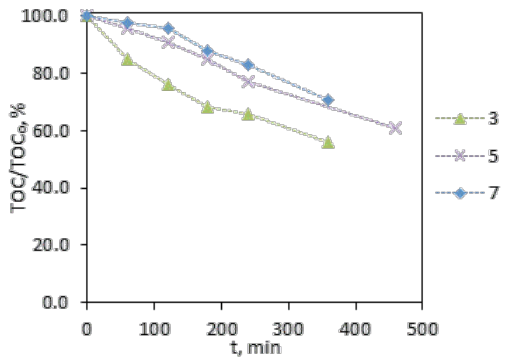

Figure 10: Effect of the initial pH on the paraquat mineralization using deposit P12 (with no pH re-adjustment after deposit addition) (T = 30 ºC, $[PQ]_0 = 3.98 \times 10^{-4}$ M, $[H_2O_2]_0 = 1.5 \times 10^{-2}$ M, [P12] = 118.6 mg/L and [Fe] = 1.0×10^{-3} M).

Using a specific pH of 5, different experiments were then carried out: (1) with pH adjustment only before adding the deposit and no further re-adjustment, (2) with re-adjustment after the deposit addition and before insertion of H_2O_2 in the reactor, and (3) using a buffer. The buffer used was prepared according to Vogel (1961): using 3.0 mL of 0.2 M acetic acid and 7.0 mL of 0.2 M sodium acetate, creating a solution with a final pH of 4.99. It should be noticed that the buffer used is organic, being susceptible of being degraded by the hydroxyl radicals.

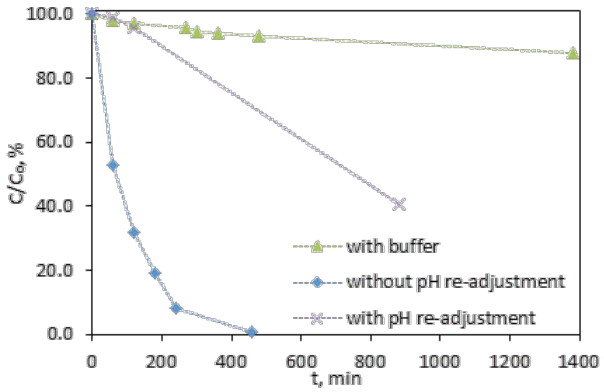

Figure 11: Study of the paraquat degradation along the oxidation using deposit P12 and different methods of pH adjustment (T = 30 ºC, $pH_0 = 5.0$, $[PQ]_0 = 3.98 \times 10^{-4}$ M, $[H_2O_2]_0 = 1.5 \times 10^{-2}$ M, [P12] = 118.6 mg/L and [Fe] = 1.0×10^{-3} M).

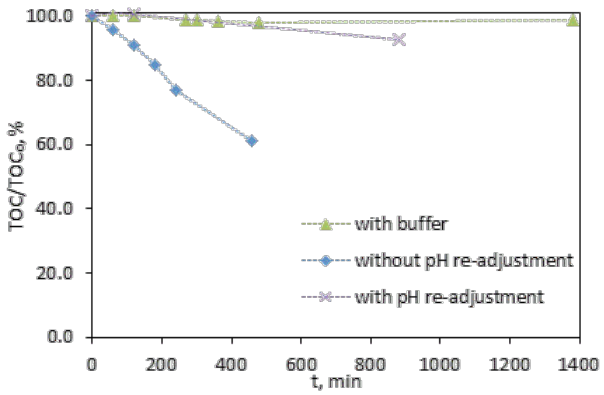

Figure 12: Study of the paraquat mineralization along the oxidation using deposit P12 and different methods of pH adjustment (T = 30 ºC, pH_0 = 5.0, $[PQ]_0 = 3.98 \times 10^{-4}$ M, $[H_2O_2]_0 = 1.5 \times 10^{-2}$ M, [P12] = 118.6 mg/L and [Fe] = 1.0×10^{-3} M).

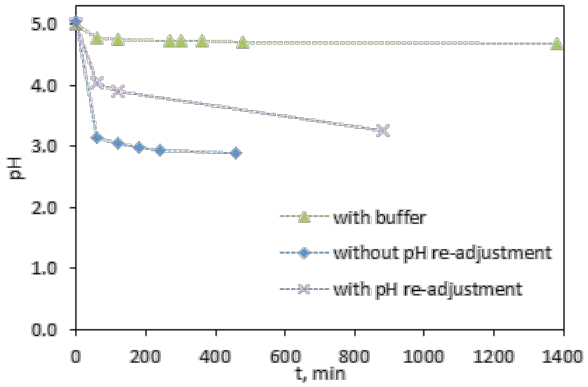

Figure 13: pH evolution along the oxidation using deposit P12 and different methods of pH adjustment (T = 30 ºC, pH_0 = 5.0, $[PQ]_0 = 3.98 \times 10^{-4}$ M, $[H_2O_2]_0 = 1.5 \times 10^{-2}$ M, [P12] = 118.6 mg/L and [Fe] = 1.0×10^{-3} M).

Figure 11 and Figure 12 show that when the pH is not re-adjusted, far better degradation and mineralization performances are reached. The reason is related with the pH decrease as the oxidation proceeds, reaching values close to 3 after ca. 1 h of oxidation (Figure 13). As long as the buffer is used, pH remains close to 5, yielding a much smaller catalytic activity (Figure 11 and Figure 12). The decrease of the pH due to the formation of acid products (like carboxylic acids) along oxidation and/or to the acid character of the solid made the pH control difficult (Figure 13), but revealed to be quite important because allowed the oxidation to proceed at high initial pH values, without requiring acidification of the medium.

1.3.6 Homogeneous vs. heterogeneous process

Figure 14 and Figure 15 compare the performances between iron sulphate and the solid deposit P12, for the same total amount of iron in solution. It is perceptible that the process with the iron sulphate salt (homogeneous process) proceeds slightly faster, either in terms of paraquat degradation or mineralization rates. Even so, final performances are similar, putting into evidence the remarkable performance of this pipe deposit.

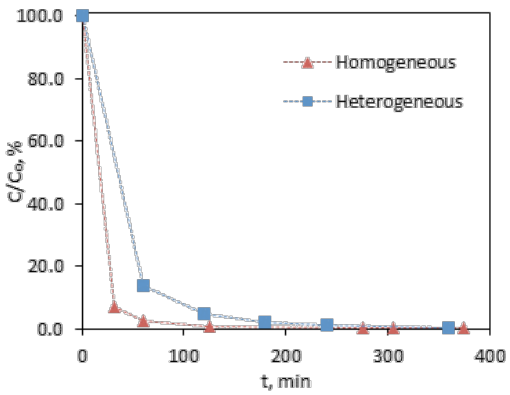

Figure 14: Comparison between the homogeneous (with ferrous iron) and heterogeneous ([P12] = 118.6 mg/L) processes in terms of paraquat degradation (T = 30 ºC, pH_0 = 3.0, $[PQ]_0 = 3.98 \times 10^{-4}$ M, $[H_2O_2]_0 = 1.5 \times 10^{-2}$ M and $[Fe]_0 = 1.0 \times 10^{-3}$ M).

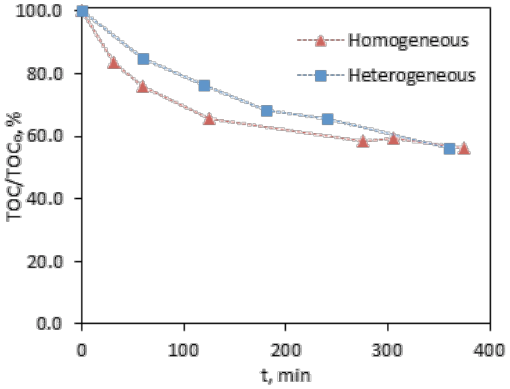

Figure 15: Comparison between the homogeneous (with ferrous iron) and heterogeneous ([P12] = 118.6 mg/L) processes in terms of paraquat mineralization (T = 30 ºC, pH_0 = 3.0, $[PQ]_0 = 3.98 \times 10^{-4}$ M, $[H_2O_2]_0 = 1.5 \times 10^{-2}$ M and $[Fe]_0 = 1.0 \times 10^{-3}$ M).

Aiming evaluating the contribution of the homogeneous Fenton process that might result from the leached iron in the run employing deposit P12, Fe concentration in solution was measured along time. Figure 16 shows the results obtained, being evident that the concentration increases along time. Still, the concentration of dissolved iron is high for short reaction times, yielding an average value along the experiment of 21.7 mg/L. A homogeneous experiment was then carried out starting with an iron (II) salt dose of 3.9×10^{-4} M (21.7 mg/L). This assay is compared in Figure 17 and Figure 18 with the performance of the solid, which is clearly better. So, leached iron cannot explain the results attained with this deposit.

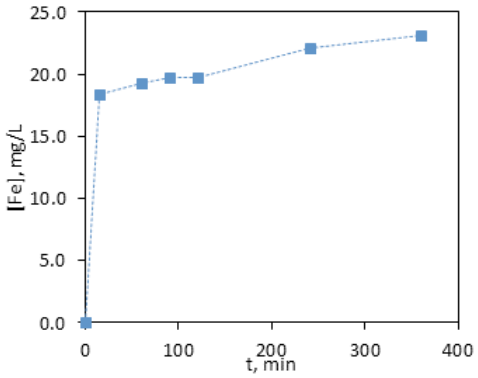

Figure 16: Soluble iron concentration along the reaction using deposit P12 (T = 30 ºC, pH_0 = 3.0, $[PQ]_0$ = 3.98 × 10^{-4} M, $[H_2O_2]_0$ = 1.5 × 10^{-2} M, [P12] = 118.6 mg/L and [Fe] = 1.0 × 10^{-3} M).

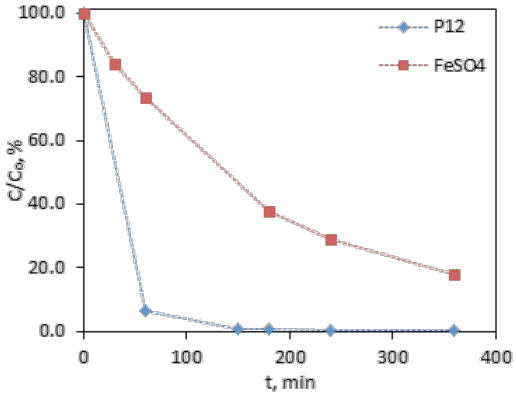

Figure 17: Paraquat degradation using as catalysts solid P12 (heterogeneous process, [P12] = 118.6 mg/L) or an iron salt ($FeSO_4$ – homogeneous process) (T = 30 ºC, pH_0 = 3.0, $[PQ]_0$ = 3.98 × 10^{-4} M, $[H_2O_2]_0$ = 1.5 × 10^{-2} M and [Fe(P12)] = 1.0 × 10^{-3} M *vs.* [Fe (II)] = 3.9 × 10^{-4} M).

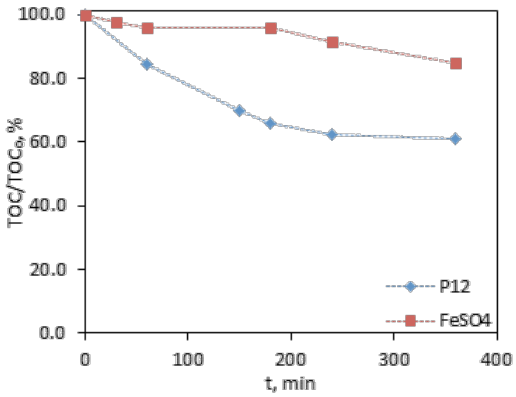

Figure 18: Paraquat mineralization using as catalysts solid P12 (heterogeneous process, [P12] = 118.6 mg/L) or an iron salt ($FeSO_4$ – homogeneous process) (T = 30 ºC, pH_0 = 3.0, $[PQ]_0$ = 3.98 × 10^{-4} M, $[H_2O_2]_0$ = 1.5 × 10^{-2} M and [Fe(P12)] = 1.0 × 10^{-3} M *vs.* [Fe (II)] = 3.9 × 10^{-4} M).

To assure if there are other dissolved metals that can have a role in the catalytic process, experiments with the leached ions from the most promising deposits were performed: the deposits P12 and APP1 were thus continuously stirred with paraquat, in a medium pH of 3 at 30 ºC, for 6 hours; then, this suspension was filtered to remove the solids and hydrogen peroxide added to the

filtered solution, initiating the Fenton's process (it should however be remarked that with this approach all ions leached during the process are initially present in the reaction mixture, thus accelerating the process). The results can be found in Figure 19 and Figure 20. According to Figure 19, deposit P12 shows a similar catalytic performance as the leached ions (homogeneous run, employing the filtrate), being evident that the metals that leached out from the solid and are present in the liquid phase are also responsible for the catalytic activity. This can be explained by the fact that apart from iron, many other metals, and particularly transition metals, catalyse the Fenton's reaction. The leached metals concentration was measured and it was found that the solution is quite complex, as is the solid. However, the main metal found in solution was clearly iron – about 38% of the iron contained in the deposit was leached, but the contribution from all other ions cannot be ruled out.

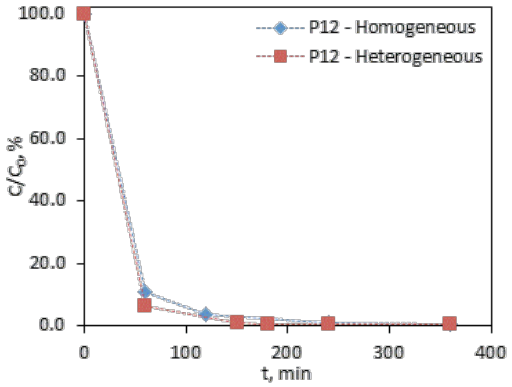

Figure 19: Evaluation of paraquat degradation using deposit in suspension *vs* leached ions that result from deposit P12. ([P12] = 118.6 mg/L, T = 30 ºC, pH_0 = 3, $[PQ]_0 = 3.98 \times 10^{-4}$ M, $[H_2O_2]_0 = 1.5 \times 10^{-2}$ M and [Fe] = 1.0×10^{-3} M, when deposits are used).

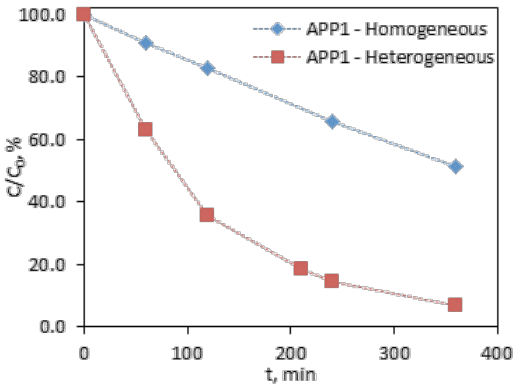

Figure 20: Evaluation of paraquat degradation using deposit in suspension *vs* leached ions that result from deposit APP1. ([APP1] = 136.8 mg/L, T = 30 ºC, pH_0 = 3, $[PQ]_0 = 3.98 \times 10^{-4}$ M, $[H_2O_2]_0 = 1.5 \times 10^{-2}$ M and [Fe] = 1.0×10^{-3} M, when deposits are used).

The performance of deposit APP1, and that of the corresponding leached ions, is shown in Figure 20. It can be seen that in this case the oxidation using the solid has a far better catalytic performance than the leached ions. In the case of deposit APP1 the main metal found in solution was also iron, while the other metals were found in residual concentrations (as could be anticipated

based on the solids composition).

It can thus be concluded that depending on the solid nature and properties, the catalytic performance can be predominantly due to the presence of the solid phase (APP1), but in some cases the homogenous process resulting from leached ions plays an important role (P12). In any case, the pipe deposits can be used as catalysts for paraquat degradation.

1.4 Conclusions

It was evidenced the possibility of using some pipe deposits taken from water networks as catalysts in the peroxidation of paraquat (Fenton-like process); the process is essentially catalytic, being negligible the role of adsorption. However, the contribution of the homogeneous process by dissolved iron and other ions depends on the type of deposit used. The deposits are quite complex and the reasons for their completely different performances are not yet completely clear. Even so, it is anticipated that the iron oxides present in each one play a role, because the XRD diffractograms evidenced the presence of different oxides in each sample, although the presence of other metals should not be ruled out. The pH_{pzc} of the deposits is also of concern, as they inherently affect the medium pH when the deposits are added to a paraquat solution.

For the solids tested, the effect of particle size is almost negligible. A better degradation is achieved when the pH of 3.0 is used. Nevertheless, the possibility of using higher pHs was evidenced, up to values of at least 7, due to the acidification of the water along oxidation/solids addition.

The results obtained show that, depending on the types of solids present in a given water network, in situ treatment can be made without insertion of chemicals apart from the oxidant, in case of a contamination event.

2 Efficacy of Fenton reaction for removal of paraquat pesticide in a pilot plant

The present section intends to evaluate the efficacy of the Fenton-like reaction for the elimination of paraquat present in water in a pilot plant. For this purpose, some preliminary assays using ferrous iron were performed (homogeneous process) and then compared with experiments where steel pipes were used and also iron rich loose deposits (heterogeneous process). According to the aim of the SecurEau, the study of the decontamination procedure in a pilot plant is of huge interest, once the decontamination is made *in situ* and it also makes possible to take some advantage of the deposits present along the pipe networks as catalysts.

2.1 Introduction

Advanced oxidation processes (AOP's) are known to be very effective to treat wastewaters (Neyens and Baeyens, 2003). These processes consist in the formation of highly reactive and non-selective species - hydroxyl radicals (E_0= 2.8 V). The organic compounds are oxidized by these radicals and mineralized into water, carbon dioxide and mineral salts.

The AOP studied herein was the Fenton's reaction, which is, as above-mentioned, based on the generation of hydroxyl radicals ($^{\cdot}OH$) through the reaction between ferrous ions (Fe^{2+}) and hydrogen peroxide (H_2O_2) and the subsequent reaction between these radicals and the organic matter, according to the reactions (1) to (3), of page 1.

Although being an efficient process, the acidic medium required (pH between 2 and 4), the high amounts of iron sludge created and the required neutralization of the treated solutions before disposal are recognized as the main constrains to this methodology (Shukla *et al.*, 2010). As an alternative to the homogeneous oxidation, heterogeneous catalysis can be used, once reactions can be performed at higher pH values and the iron is completely recovered (Herney-Ramirez *et al.*, 2010; Duarte *et al.*, 2009; Navalon *et al.*, 2010). This type of processes brings important advantages, being the main ones the easy separation of the catalyst from the final effluent and the easy recovery, the iron immobilization avoiding the formation of iron-containing sludge.

In this section of the deliverable, the Fenton's reagent is tested to degrade the SecurEau chemical paraquat in a water distribution pilot loop. Besides, and also the performance of some loose deposits as catalysts in the Fenton's reaction are assessed, as well as steel pipes. Thus, both homogeneous and heterogeneous Fenton-like processes are tested. A preliminary study of the oxidation performance by gradual addition of peroxide was also performed.

2.2 Materials and Methods

2.2.1 Reagents

Commercial Paraquat – Gramoxone (GMX) – 32.5% (w/w) in paraquat dichloride was used and gently supplied by Syngenta. Two loose deposits, one obtained from a local water distribution system (deposit #5),

and one taken from a tank of a firefighter department (UGUNDZ), both from the city of Riga, were tested as catalysts of the Fenton-like reaction. The other reagents used are the same as mentioned in the section 1.2.1.

2.2.2 Experimental set-up

2.2.2.1 Stirred Batch Reactor (Lab scale)

The oxidation assays done in lab scale were performed as described above, in section 1.2.5.

A solution of paraquat (PQ) of concentration 3.9×10^{-4} M (100 mg/L) was used. After the solution has reached the temperature of 30ºC, the pH adjustment was done (value desired: 3.0) adding H_2SO_4 0.1 M.

After stabilization of the pH, the iron (II) salt was added to the pesticide solution. The reaction was initiated by adding a pre-established volume of H_2O_2 (time zero of the reaction).

2.2.2.2 Recirculation tubular reactor (Pilot loop)

The pilot loop used in these experiments was made of PVC pipes; however, some sections were replaced, in some experiments, by cast iron pipes, to assess if those pipes can catalyze the Fenton's reaction. The reagents (GMX, acid, hydrogen peroxide and ferrous iron) were introduced in the recirculation tubular reactor using the manual pump coupled to the system. Figure 21 shows the experimental set-up.

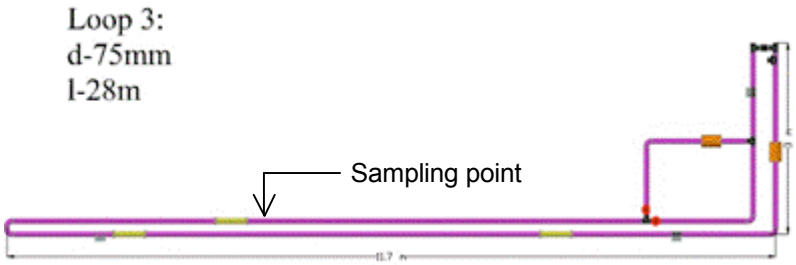

Figure 21: Illustration of the pilot loop used.

The pilot loop has a total length of 28 meters, internal diameter of 75 millimeters and the replaceable sections have a length of 0.5 m (first one) and 13.6 m (second one).

The experiments were conducted diluting a small volume of a 1 g/L PQ water solution in the pilot loop previously filled with water to reach the final concentration of PQ of 100 mg/L (3.9×10^{-4} M), followed by the addition of a certain amount of concentrated sulfuric acid to achieve the required initial pH (7 mL for 103 L of the water used, in the case of a desired pH of 3.0).

After the addition of these reagents, the solution was flowing in the recirculation loop for around one hour to assure that the homogeneous mixture was achieved. After this period of time, the ferrous iron was added to the loop and the reaction was started by adding hydrogen peroxide. Samples were taken along the reaction time and filtrated with PTFE syringe filters, with pore diameter of 0.2 µm, for further analysis using HPLC-DAD to measure the paraquat degradation, DOC (Dissolved Organic Carbon) analyzer to measure de degree of mineralization, and Atomic Absorption (AA) to measure the amount of iron in solution.

Table 2.1: Operating conditions for each experiment (Series 1).

	RUN #1	RUN #2	RUN #3	RUN #4	RUN #5
$[H_2O_2]_0$, M	1.5×10^{-2}	1.5×10^{-2}	1.5×10^{-2}	1.5×10^{-2}	1.5×10^{-2}
$[FeSO_4 \cdot 7H_2O]_0$, M	5.0×10^{-4}	5.0×10^{-4}	5.0×10^{-4}	---	5.0×10^{-4}
[deposit], mg/L	---	---	---	**128**	128
$[PQ]_0$, M	3.9×10^{-4}	3.9×10^{-4}	3.9×10^{-4}	3.9×10^{-4}	3.9×10^{-4}
pH_0	3.0	**5.0**	3.0	3.0	3.0
$T_{average}$, ºC	≈ 20	≈ 20	≈ 20	≈ 20	≈ 20
Pipes types	PVC	PVC	**PVC + cast iron, 0.5 m**	PVC	**PVC + cast iron, 0.5 m**
Iron source	Iron (II) salt	Iron (II) salt	Iron (II) salt	**Loose deposit #5**	**Iron (II) salt + loose deposit #5**

Table 2.2: Operating conditions for each experiment (Series 2).

	RUN #6	RUN #7	RUN #8	RUN #9	RUN #10
$[H_2O_2]_0$, M	1.5×10^{-2}	1.5×10^{-2} (*)	1.5×10^{-2}	1.5×10^{-2}	1.5×10^{-2} (*)
$[FeSO_4 \cdot 7H_2O]_0$, M	5.0×10^{-4}	5.0×10^{-4}	---	---	5.0×10^{-4}
[deposit], mg/L	---	---	744	---	---
$[PQ]_0$, M	3.9×10^{-4}	3.9×10^{-4}	3.9×10^{-4}	3.9×10^{-4}	3.9×10^{-4}
pH_0	3.0	3.0	3.0	3.0	3.0
$T_{average}$, ºC	≈ 20	≈ 20	≈ 20	≈ 20	≈ 20
Pipes types	PVC	PVC	PVC	**Cast iron pipe, 13.6 m**	PVC
Iron source	Iron (II) salt	Iron (II) salt	**Loose deposit UGUNDZ**	---	Iron (II) salt

(*) Gradual addition of H_2O_2.

2.2.3 Analytical methods

The paraquat degradation was followed by HPLC-DAD (High Performance Liquid Chromatography with Diode Array Detection), as mentioned in section 1.2.4. In this case, the chromatographic separation was achieved by a RP C18 Purospher® STAR column (250 mm × 4 mm, 5 µm), supplied by VWR, and paraquat was quantified at 259 nm, after 3 min of the start of the injection. This method is characterized by a detection limit of 0.58 mg/L.

2.3 Results and discussion

The operating conditions used in each experiment in the pilot loop are presented above, in Table 2.1 and Table 2.2. The conditions used were based in the conditions studied in deliverable 5.5.

A previous parametric study in a stirred batch reactor was done - cf. deliverable 5.5. The conditions which led to the best mineralization degree were T = 30 ºC, pH_0 = 3, $[H_2O_2]_0 = 1.5 \times 10^{-2}$ M and [Fe (II)] = 5.0×10^{-4} M, for a contaminant concentration $[PQ]_0 = 3.9 \times 10^{-4}$ M. For this reason, this study was performed using the same concentration values. An assay using a pH medium of 5 was also tested (Table 2.1). The average temperature in these assays was not controlled, due to the dimension of the recirculation tubular reactor; the experiments were therefore performed using room temperature (≈20ºC) in all runs. Furthermore, assays using loose deposit particles, instead of ferrous iron, were performed to assess if this solid would be enough to catalyze the process, as well as different lengths of steel pipes –Table 2.1 and Table 2.2.

The results obtained are illustrated in the figures below.

2.3.1 Stirred batch reactor (lab scale) *vs.* Recirculation tubular reactor (pilot loop)

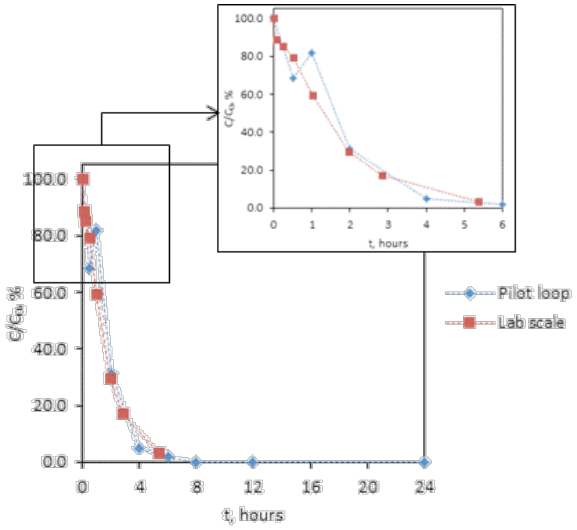

Figure 22: Commercial Paraquat degradation – comparison between the lab scale (T = 30 ºC, pH_0 = 3.0, $[PQ]_0 = 3.98 \times 10^{-4}$ M, $[H_2O_2]_0 = 1.5 \times 10^{-2}$ M, and [Fe] = 5.0×10^{-4} M), and the pilot loop (T ≈ 20 ºC, pH_0 = 3.0, $[PQ]_0 = 3.98 \times 10^{-4}$ M, $[H_2O_2]_0 = 1.5 \times 10^{-2}$ M, and [Fe] = 5.0×10^{-4} M).

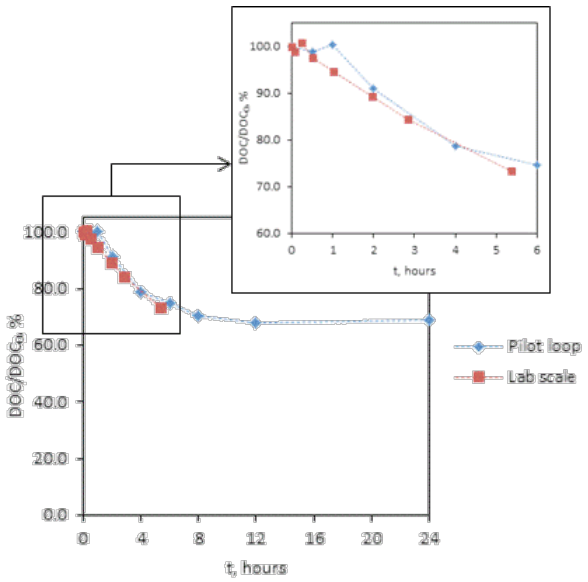

Figure 23: Commercial Paraquat mineralization – comparison between the lab scale (T = 30 ºC, pH_0 = 3.0, $[PQ]_0 = 3.98 \times 10^{-4}$ M, $[H_2O_2]_0 = 1.5 \times 10^{-2}$ M, and [Fe] = 5.0×10^{-4} M), and the pilot loop (T ≈ 20 ºC, pH_0 = 3.0, $[PQ]_0 = 3.98 \times 10^{-4}$ M, $[H_2O_2]_0 = 1.5 \times 10^{-2}$ M, and [Fe] = 5.0×10^{-4} M).

From Figure 22 and Figure 23, it can be seen that the performance of the process, for the commercial paraquat product degradation (gramoxone – GMX), in both reactors is very similar, which allow us to infer that the conditions used in the pilot loop (particularly lower temperature – 20 ºC) does not influence the process, being very effective in real conditions.

2.3.2 Effect of the initial pH

To assess the effect of the pH in the performance of PQ degradation, two experiments were performed and compared. RUN #1 shows the PQ degradation when an initial pH of 3.0 is used and it is compared with RUN #2, which shows the PQ degradation when an initial pH of 5.0 is used (cf. Table 2.1). The results are presented in Figure 24 to Figure 27.

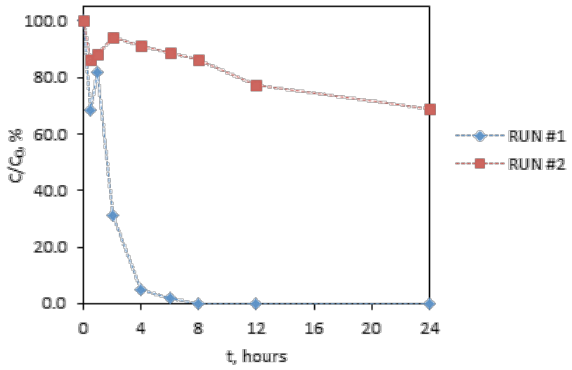

Figure 24: Effect of the initial pH in the PQ degradation (T ≈ 20 ºC, $[PQ]_0 = 3.98 \times 10^{-4}$ M, $[H_2O_2]_0 = 1.5 \times 10^{-2}$ M, and [Fe] = 5.0×10^{-4} M).

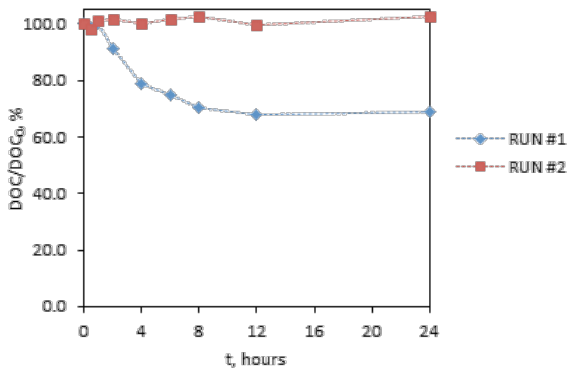

Figure 25: Effect of the initial pH in the PQ mineralization (T ≈ 20 ºC, $[PQ]_0 = 3.98 \times 10^{-4}$ M, $[H_2O_2]_0 = 1.5 \times 10^{-2}$ M, and [Fe] = 5.0×10^{-4} M).

RUN #1 and RUN #2 have the same source of iron – Iron (II) salt – and as it can be seen in Figure 27, the evolution of total iron concentration is similar for both experiments; however, there are differences in the soluble iron concentration, once the initial pH is different and it affects the solubility of the iron from the salt; therefore, and as expected, soluble iron is higher for more acidic conditions. The evolution of pH can be seen in Figure 26.

From Figure 24 and Figure 25 it can also be seen that the initial pH has a big impact in the catalytic process, once at the initial pH 5 no mineralization was achieved and only 30% of degradation was reached in 24 h, while for the initial pH of 3 the degradation was complete after 8 hours of reaction, and after 24h a mineralization of 30% of the pesticide was achieved.

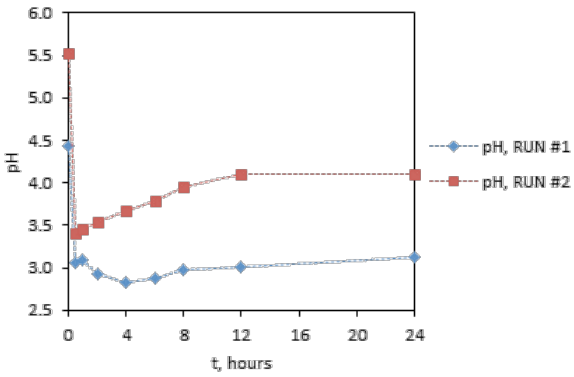

Figure 26: pH evolution along time (T ≈ 20 ºC, $[PQ]_0 = 3.98 \times 10^{-4}$ M, $[H_2O_2]_0 = 1.5 \times 10^{-2}$ M, and [Fe] = 5.0×10^{-4} M).

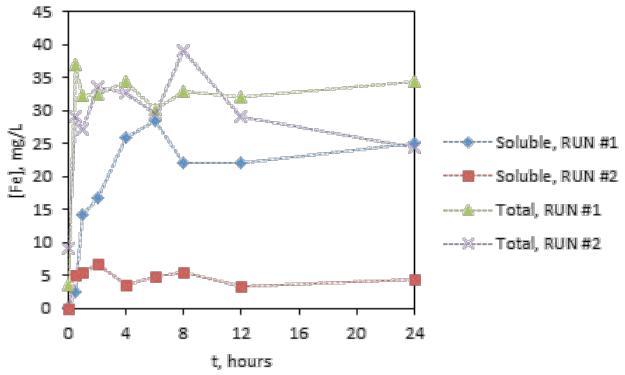

Figure 27: Iron concentration along time of reaction for both experiments (T ≈ 20 ºC, $[PQ]_0 = 3.98 \times 10^{-4}$ M, $[H_2O_2]_0 = 1.5 \times 10^{-2}$ M, and [Fe] = 5.0×10^{-4} M).

From Figure 27, it can be seen that almost no soluble iron is present in the reaction using an initial pH of 5 – RUN #2 – because at high pH values, the iron present is converted into ferric iron, which precipitates, becoming not available to react with the hydrogen peroxide and catalyze the process.

2.3.3 Steel pipe as catalyst – influence of the length

From the analysis of Figure 28 and Figure 29 it can be seen that the better performance is achieved in RUN #9, which uses a larger cast iron pipe section (13.6 m) and no iron salt, whereas in RUN #3 a shorter cast iron pipe section (0.5 m) is used and ferrous iron is added; in RUN #1 only ferrous iron salt was included in the loop.

From this observation, in can thus be concluded that cast iron pipes catalyse the Fenton's process and also that the effect of the cast iron pipe length has an important influence in the process. In such conditions, no iron salt might inclusively be needed to add to the process, still allowing to completely degrade paraquat as occurs in RUN #9.

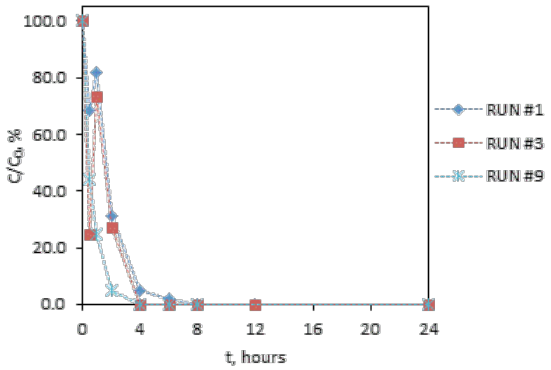

Figure 28: PQ degradation – RUN #1 (with ferrous iron), RUN #3 (ferrous iron and 0.5 m cast iron pipe) and RUN #9 (13.6 m cast iron pipe) – operating conditions shown in Table 2.1 and Table 2.2.

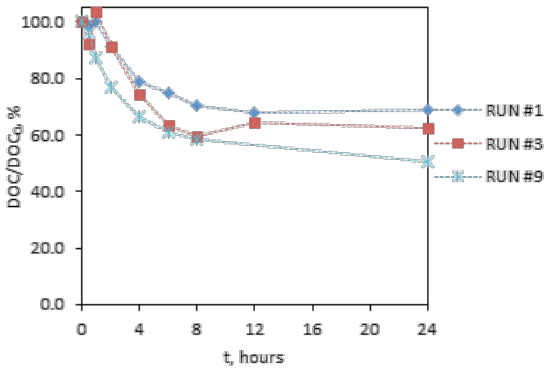

Figure 29: PQ mineralization – RUN #1 (with ferrous iron), RUN #3 (ferrous iron and 0.5 m cast iron pipe) and RUN #9 (13.6 m cast iron pipe) – operating conditions shown in Table 2.1 and Table 2.2.

One should notice, from Figure 28 to Figure 30, that when the medium pH starts increasing, the degradation and also the mineralization achieves a *plateau*, which suggests that all the peroxide might be consumed and no reaction occurred further. The increase in the pH value may be related with the release of the dissolved carbon dioxide present in the water.

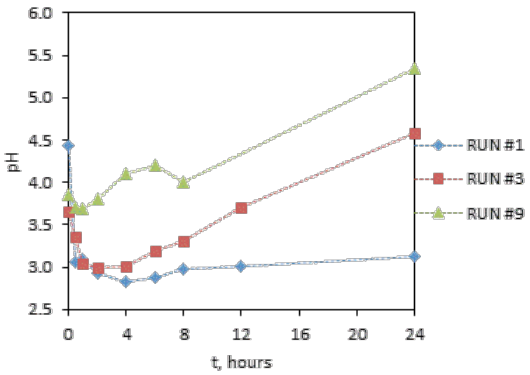

Figure 30: Evolution of the pH along the reaction of PQ degradation – RUN #1 (with ferrous iron), RUN #3 (ferrous iron and 0.5 m cast iron pipe) and RUN #9 (13.6 m cast iron pipe) – operating conditions shown in Table 2.1 and Table 2.2.

Comparing RUN #1 and RUN #3 in terms of the total iron concentration present in the water, from Figure 31 it can be concluded that in RUN #3 such parameter is slightly higher than in RUN #1, particularly after 12 h of reaction, but for the soluble iron the final concentrations are similar.

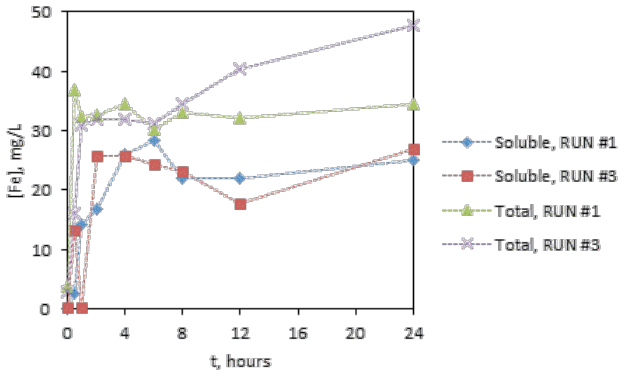

Figure 31: Iron concentration along the PQ degradation – RUN #1 (with ferrous iron), RUN #3 (ferrous iron and 0.5 m cast iron pipe) and RUN #9 (13.6 m cast iron pipe) – operating conditions shown in Table 2.1and Table 2.2.

The thickness of the steel pipe used in RUN #3 was also checked before and after the experiment to assess if there was some kind of release of iron into the liquid phase – the same must be done for RUN #9 soon. This measurement was done by sonication, and using 4 different points of the pipe. In normal conditions, for the steel pipe, the thickness reduction along time would be around 160 nm/day; using this harsh conditions (pH = 3 and hydrogen peroxide concentration = 1.5×10^{-2} M), the rate of thickness reduction calculated was 7.5 µm/day, thus explaining the results reported in Figure 31. Once this pipe has a thickness of 7.5 mm, and if these conditions were observed permanently, this pipe should be replaced only after 2.5 years of use.

2.3.4 Loose deposits as catalysts

Two deposits, as mentioned in section 2.2.1, were tested as catalysts in this process. Further characterization of the deposits must be done in order to better understand the results obtained along this study.

RUN #1 shows the degradation process in the presence of ferrous iron, RUN #4 presents the oxidation in the presence of the deposit #5 and RUN #8 shows the performance in the presence of the deposit UGUNDZ. The iron content of each deposit is unknown (further analysis will provide this information); the iron concentration of 5.0×10^{-4} M used in RUN #1 is provided by the addition of the ferrous iron salt.

Analysing Figure 32 and Figure 33 it can be said that the process is more effective when using the ferrous iron (RUN #1); RUN #4 yielded no paraquat degradation neither mineralization, but RUN #8 shows some mineralization and degradation. This evidences the possibility of using some pipe deposits as catalysts of the Fenton's process, which performance depends on the deposit used, in agreement with the results shown in section 1 of this deliverable. However, this was now proved in a pilot-scale reactor.

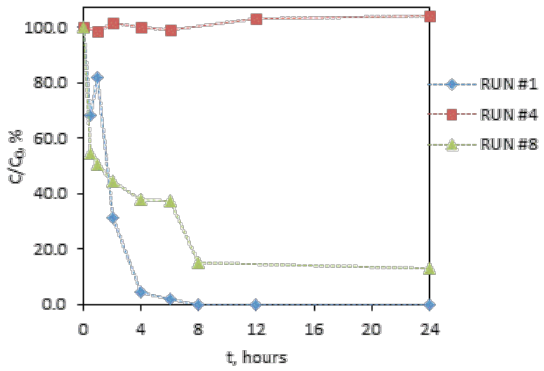

Figure 32: PQ degradation – RUN #1 (ferrous iron), RUN #4 (128 mg/L deposit #5) and RUN #8 (744 mg/L deposit UGUNDZ) – operating conditions shown in Table 2.1 and Table 2.2.

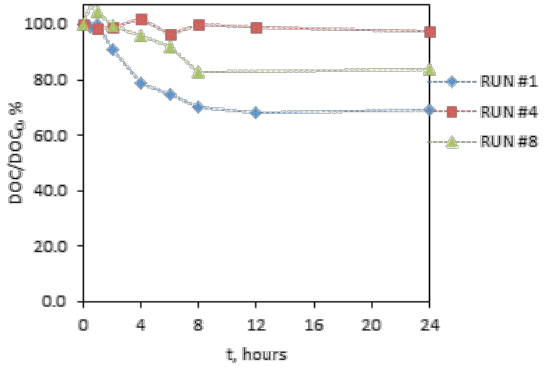

Figure 33: PQ mineralization – RUN #1 (ferrous iron), RUN #4 (128 mg/L deposit #5) and RUN #8 (744 mg/L deposit UGUNDZ) – operating conditions shown in Table 2.1 and Table 2.2.

It is of big interest to understand the evolution of the pH along time (Figure 34); as said before, the increase in the pH medium corresponds to the achievement of a *plateau* in the degradation and mineralization data; this can be explained by the availability of the ferrous iron to react with the peroxide. Once the ferrous iron is precipitated, no more iron is available to react with the peroxide and thus no radicals are generated. Besides, upon increasing the medium pH the peroxide is decomposed, once it is very unstable, into oxygen and water. All these issues decrease reaction performance. On the other hand, the increase in the pH along the reaction can be related with the pH_{pzc} of the deposit, as seen in section 1.

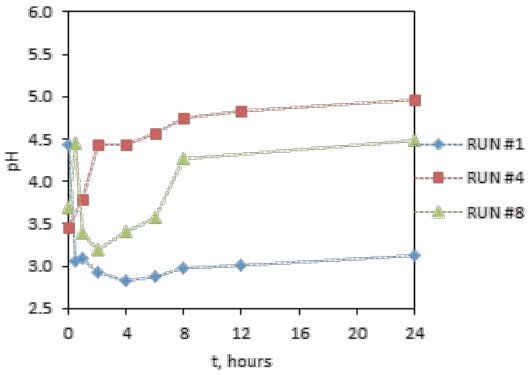

Figure 34: Evolution of the pH along the reaction of PQ degradation – RUN #1 (ferrous iron), RUN #4 (128 mg/L deposit #5) and RUN #8 (744 mg/L deposit UGUNDZ) – operating conditions shown in Table 2.1 and Table 2.2.

The above results are also in line with the dissolved iron, which is much lower for RUN #4, where reaction pH is higher (cf. Figure 34 and Figure 35).

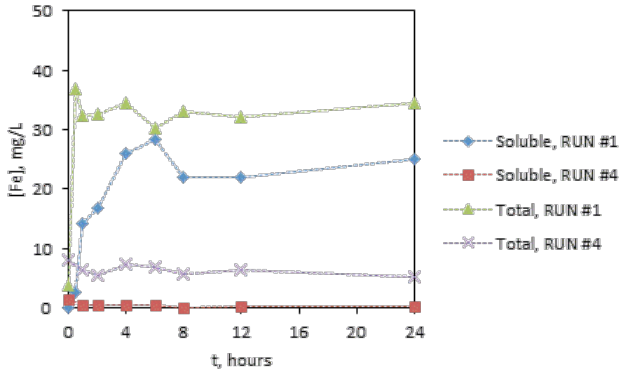

Figure 35: Iron concentration along time – RUN #1 (ferrous iron), RUN #4 (128 mg/L deposit #5) and RUN #8 (744 mg/L deposit UGUNDZ) – operating conditions shown in Table 2.1 and Table 2.2.

2.3.5 Effect of the gradual addition of hydrogen peroxide in the oxidation process

The gradual addition of H_2O_2 was also tested. The experiments are compared in Figure 36 and Figure 37, and the way of addition of the oxidant is shown in Table 2.3. All other experimental conditions are the same (cf. Tables 2 and 3).

Table 2.3: Way of H_2O_2 addition.

	Volume of H_2O_2, mL		
Time, h	RUN #1	RUN #7	RUN #10
0	~ 160	32	15
2	---	32	15

4	---	32	30
6	---	32	30
8	---	32	70

As can be seen in Figure 36 and Figure 37, in the case of progressive addition of the oxidant (RUN #7 and RUN #10) the performance is worse in the first hours than for RUN #1 due to a slower reaction rate (as expected, because initial oxidant dose is smaller). However, after 24 hours of reaction, Figure 37 illustrates that it was achieved a better mineralization degree (as a consequence of the decreased parallel and undesired reactions that are favoured by a higher H_2O_2 concentration – e.g., scavenging of radicals). This run proves that a higher H_2O_2 utilization efficiency is achieved with this gradual addition, as also shown in previous works (Santos *et al.*, 2011). One should note also that for RUN #10 the final mineralization degree is even bigger that for the RUN #7, once the gradual addition in RUN #10 was made with increasing amounts of peroxide.

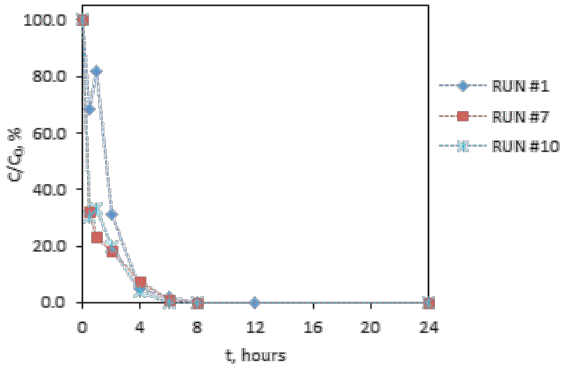

Figure 36: Effect of the gradual addition of H_2O_2 in the performance of PQ degradation (T ≈ 20 ºC, $[PQ]_0$ = 3.98 × 10^{-4} M, $[H_2O_2]_0$ = 1.5 × 10^{-2} M, and [Fe] = 5.0 × 10^{-4} M).

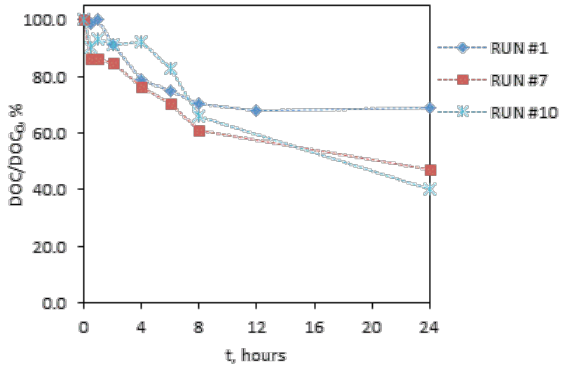

Figure 37: Effect of the gradual addition of H_2O_2 in the performance of PQ mineralization (T ≈ 20 ºC, $[PQ]_0$ = 3.98 × 10^{-4} M, $[H_2O_2]_0$ = 1.5 × 10^{-2} M, and [Fe] = 5.0 × 10^{-4} M).

2.4 Conclusions

The results show that paraquat degradation can be done in the pilot loop, achieving similar results to those obtained in lab scale reactor, i.e., homogeneous Fenton's reaction is an effective process in both scales for the pesticide degradation.

Loose deposits can be used as catalysts, but special care must be taken to their composition, as well as the amount used / present in water pipes. The same can be said about the cast iron pipes – the size of metallic pipes has a big influence in the oxidation process; the larger the pipe, the bigger is the contribution in the heterogeneous process, but special attention is required to measure the decrease in the thickness of those pipes for long term use, once they can be solubilized.

The gradual addition of hydrogen peroxide showed to be the best option in the oxidation process, allowing reaching higher mineralization degrees.

It is of big importance to highlight that, according to the results obtained in this study, it is possible to decontaminate water in a real water network by advanced Fenton oxidation. Besides, it is also possible to run the process efficiently using either the cast iron pipes or the loose deposits as the catalyst iron source.

2.5 References

APHA, AWWA, WEF, Standard Methods for the Examination of Water and Wastewater, 20th ed., American Public Health Association, American Water Works Association, Water Pollution Control Federation, Washington, DC, 1998.

Bigda, R.J. Consider Fenton´s chemistry for wastewater treatment, Chem. Eng. Prog., 91 (1995) 62-66.

Duarte, F., Madeira, L.M. Fenton- and photo-Fenton-like degradation of a textile dye by heterogeneous processes with Fe/ZSM-5 zeolite, Sep. Sci. Technol., 45 (2010) 1512-1520.

Duarte, F., Maldonado-Hódar, F.J., Madeira, L.M. Influence of the characteristics of carbon materials on their behaviour as heterogeneous Fenton catalysts for the elimination of the azo dye Orange II from aqueous solutions, Appl. Catal. B, 103 (2011) 109-115.

Duarte, F., Maldonado-Hódar, F.J., Pérez-Cadenas, A.F., Madeira, L.M. Fenton-like degradation of azo-dye Orange II catalyzed by transition metals on carbon aerogels, Appl. Catal. B, 85 (2009) 139-147.

Dükkanci, M., Gündüz, G., Yilmaz, S., Prihod'ko, R.V. Heterogeneous Fenton-like degradation of Rhodamine 6G in water using CuFeZSM-5 zeolite catalyst prepared by hydrothermal synthesis, J. Hazard. Mater., 181 (2010) 343-350.

Echeverría, F., Castaño, J., Arroyave, C., Peñuela, G., Ramírez, A., Morató, J. Characterization of deposits formed in a water distribution system, Rev. Chil. Ing., 17 (2009) 275-281.

Feng, J., Hu, X., Yue, P.L., Zhu, H.Y., Lu, G.Q. Discoloration and mineralization of reactive Red HE-3B by heterogeneous photo-Fenton reaction, Water Res., 37 (2003) 3776-3784.

Fontecha-Cámara, M.A., Álvarez-Merino, M.A., Carrasco-Marín, F., López-Ramón, M.V., Moreno-Castilla, C. Heterogeneous and homogeneous Fenton processes using activated carbon for the removal of the herbicide amitrole from water, Appl. Catal., B, 101 (2011) 425-430.

Garrido-Ramírez, E.G., Theng, B.K.G., Mora, M.L. Clays and oxide minerals as catalysts and nanocatalysts in Fenton-like reactions — A review, Appl. Clay Sci., 47 (2010) 182-192.

Hassan, H., Hameed, B.H. Fe–clay as effective heterogeneous Fenton catalyst for the decolorization of Reactive Blue 4, Chem. Eng. J., 171 (2011) 912-918.

Herney-Ramirez, J., Vicente, M.A., Madeira, L.M. Heterogeneous photo-Fenton oxidation with pillared clay-based catalysts for wastewater treatment: a review, Appl. Catal. B, 98 (2010) 10-26.

Klamerth, N., Malato, S., Maldonado, M.I., Agüera, A., Fernández-Alba, A.R. Application of photo-Fenton as a tertiary treatment of emerging contaminants in municipal wastewater, Environ. Sci. Technol., 44 (2010) 1792-1798.

Kusić, H., Koprivanac, N., Selanec, I. Fe-exchanged zeolite as the effective heterogeneous Fenton-type catalyst for the organic pollutant minimization: UV irradiation assistance. Chemosphere, 65 (2006) 65-73.

Lu, M.C., Chen, J.N., Chang, C.P. Effect of inorganic ions on the oxidation of dichlorvos insecticide with Fenton's reagent, Chemosphere, 35 (1997) 2285-2293.

Matta, R., Hanna, K., Chiron, S. Fenton-like oxidation of 2,4,6-trinitrotoluene using different iron minerals, Sci. Total Environ., 385 (2007) 242-251.

Navalon, S., Alvaro, M., Garcia, H. Heterogeneous Fenton catalysts based on clays, silicas and zeolites, Appl. Catal. B, 99 (2010) 1-26.

Neyens, E., Baeyens, J. A review of classic Fenton's peroxidation as an advanced oxidation technique. Journal of Hazardous Materials, 98 (2003) 33-50.

Nguyen, T.D., Phan, N.H., Do, M.H., Ngo, K.T. Magnetic Fe2MO4 (M:Fe, Mn) activated carbons: Fabrication, characterization and heterogeneous Fenton oxidation of methyl orange, J. Hazard. Mater., 185 (2011) 653-661.

Pérez, M., Torrades, F., Doménech, X., Peral, J. Fenton and photo-Fenton oxidation of textile effluents, Water Res., 36 (2002) 2703-2710.

Ramirez, J.H., Costa, C.A., Madeira, L.M., Mata, G., Vicente, M.A., Rojas-Cervantes, M.L., Lopez-Peinado, A.J., Martin-Aranda, R.M. Fenton-like oxidation of Orange II solutions using heterogeneous catalysts based on saponite clay, Appl. Catal. B, 71 (2007) 44-56.

Ramirez, J.H., Duarte, F.M., Martins, F.G., Costa, C.A., Madeira, L.M. Modelling of the synthetic dye Orange II degradation using Fenton's reagent: From batch to continuous reactor operation, Chem. Eng. J., 148 (2009) 394-404.

Rivera-Utrilla, J., Bautista-Toledo, I., Ferro-Garcia, M.A., Moreno-Castilla, C. Activated carbon modifications by adsorption of bacteria and their effect on aqueous lead adsorption, J. Chem. Technol. Biotechnol., 76 (2001) 1209-1215.

Rodrigues, C.S.D., Madeira, L.M., Boaventura, R.A.R. Optimization of the azo dye Procion Red H-EXL degradation by Fenton's reagent using experimental design, J. Hazard. Mater., 164 (2009) 987-994.

Santos, M.S.F., Alves, A., Madeira, L.M. Paraquat removal from water by oxidation with Fenton's reagent, Chem. Eng. J., 175 (2011) 279-290.

Shukla, P., Wang, S., Sun, H., Ang, H.M., Tadé, M. Adsorption and heterogeneous advanced oxidation of phenolic contaminants using Fe loaded mesoporous SBA-15 and H2O2. Chemical Engineering Journal, 164 (2010) 255-260.

Tekbas, M., Yatmaz, H.C., Bektas, N. Heterogeneous photo-Fenton oxidation of reactive azo dye solutions using iron exchanged zeolite as a catalyst. Micropor. Mesopor. Mat., 115 (2008) 594-602.

Vogel, A. A text-book of quantitative inorganic analysis including elementary instrumental analysis, 3rd ed., Longmans, London (1961).

Walling, C. Fenton's Reagent Revisited, Acc. Chem. Res., 8 (1975) 125-131.

Wekesa, M., Habtewold, A., Mirdaniali, J. Stabilization of manganese (Mn)-induced peroxide decomposition, Afr. J. Pure Appl. Chem., 5 (2011) 176-180.

Wekesa, M., Ni, Y. Mechanism of hydrogen peroxide decomposition by manganese dioxide, Tappi J., 2 (2003) 23-26.

3 Using of Fenton reaction for inactivation of *B. subtilis* spores in water

3.1 Introduction

Commonly used oxidants react directly with the outer membrane or coat of bacterial cells and spores. Strong oxidants (like chlorine) are effective but also very highly reactive with organic (like natural organic matter) and inorganic materials, thus causing formation of disinfection by-products and promoting corrosion. Classic and modified Fenton reaction showed to be effective for inactivation of *Bacillus* spp. spores (Sagripanti, 1992; Sagripanti and Bonifacino, 1996; Cross et al., 2003; (Shapiro et al., 2004). Also some studies concern photo-assisted Fenton reaction (Bandala, 2009; Bandala et al., 2011). The main advantage of the Fenton reaction is the complete destruction of contaminants to harmless compounds, e.g. CO_2, water and inorganic salts (Neyens and Baeyens, 2003). Fenton reaction targets the interior of the spore (Cross et al., 2003). The basic mechanism of Fenton reaction:

$$Fe^{3+} + H_2O_2 \rightarrow Fe^{2+} + HOO^{\bullet} + H^{+} \quad (9)$$

$$Fe^{2+} + H_2O_2 \rightarrow Fe^{3+} + HO^{\bullet} + HO^{-} \quad (10)$$

Transition metal ion is cycled between upper and lower oxidation state by its interaction with hydrogen peroxide. Basically, transition metal ion works as a catalytic agent for forming hydroxyl and other reactive free radicals. Subsequent reactions of hydroxyl radical with organic molecules include hydrogen abstraction, addition reaction to double bonds and oxidation reactions.

Ascorbic acid (AA) has long been recognized as an efficient free radical scavenger (Niki, 1991), but under certain conditions of high concentration and the presence of transition metals and dissolved oxygen, it can function as a prooxidant (Herbert, 1996). At high concentrations of AA, copper(II) is rapidly reduced to copper(I) with the formation of oxidized form of AA, dehydroascorbic acid (DAA). In biological systems copper chemically complexes with DNA or RNA. Under aerobic conditions copper(I) is oxidized back to copper(II) with the subsequent formation of hydrogen peroxide through the superoxide intermediate (Muranaka et al, 1997):

$$2Cu^{+} + 2O_2(aq) \rightarrow 2Cu^{2+} + O_2^{-} \quad (11)$$

$$2O_2^{-} + 2H^{+} \rightarrow H_2O_2 + O_2 \quad (12)$$

the net reaction being:

$$AA + O_2 \xrightarrow{Cu^{2+}} H_2O_2 + DAA \quad (13)$$

Under conditions of excess AA, where Cu^{II} in continually being reduced by AA to Cu^{I}, dissolved oxygen is converted to hydrogen peroxide. The peroxide is subsequently converted to hydroxyl

radicals by Fenton reaction (Muranaka et al, 1997):

$$Cu^{1} + H_2O_2 \rightarrow HO^{\bullet} + HO^{-} + Cu^{II} \quad (14)$$

Fenton-based disinfection using hydrogen peroxide can be more efficient with essentially no side effects compared to chlorine and glutaraldehyde (Sagripanti, 1992).

3.2 Materials and methods

3.2.1 *B. subtilis* spore preparation and selection

B. subtilis ATCC 6051 firstly were plated on the Luria Bertani (LB) agar broth. Bacterial colonies were inoculated into sterile phosphate saline buffer (7 mM Na_2HPO_4, 3 mM NaH_2PO_4, 130 mM NaCl, pH 7.2). After 6 day incubation period in 37°C the suspension was stained with malachite green and safranine to ensure the presence of the spores (about 98%). To eliminate the rest of vegetative bacteria heat shock (10 min at 80°C) was used. Afterwards the suspension was cooled and stored at 4°C.

3.2.2 The cultivation of *B. subtilis* cells

Water sample was heat shocked at 80°C for 10 min to kill the other bacteria present in the water. Serial dilutions of the samples were done when it was needed. Afterwards the 0.1 ml of sample was placed on the R2A agar plates and stored at 30°C. The evaluation of colony forming units (CFU) was done after 18-20h.

3.2.3 Reagents

Hydrogen peroxide solution (30% v/v), iron (II) sulphate heptahydrate (99.5%) and anhydrous sodium sulphite were purchased from AppliChem (Germany). Analytical grade $CuCl_2$ and Sulphuric acid (96%) were used (Poland).

3.2.4 Experimental setup

Experiments were carried out in a lab scale. Drinking water from Riga city supply was filtered through 0.22 μm filter to exclude contamination of samples with other organisms. pH was corrected using H_2SO_4 if necessary (Table 3.1). *B. subtilis* spore suspension was introduced into filtered water to reach the target concentration of 10^5 CFU/ml. Afterwards metal salt and other necessary reagents (Table 3.1) was added. After the first sample was taken H_2O_2 or AA was added.

Table 3.1: Treatment approaches for inactivation of *B.subtilis* spores.

microorganism	Transition metal , mol	Catalyzer, mol	Ratio metal to catalyst	Other reagents	pH	Run #, comments
B.subtilis 6051	Fe^{2+} $2.58 \cdot 10^{-4}$	H_2O_2 $1.5 \cdot 10^{-2}$	1:20	-	4.5	1
B.subtilis 6051	Cu^{2+} $3.13 \cdot 10^{-3}$	H_2O_2 $1.47 \cdot 10^{-1}$	1:25	-	3	2
E.coli	Cu^{2+} $3.13 \cdot 10^{-3}$	H_2O_2 $1.47 \cdot 10^{-1}$	1:25	-	3	3

B.subtilis 6051	Fe^{2+} $3.6 \cdot 10^{-2}$	H_2O_2 $1.47 \cdot 10^{-2}$	1:25	-	3.15	4
B.subtilis 6051	Cu^{2+} $6.0 \cdot 10^{-2}$	AA $1.0 \cdot 10^{-1}$	1:5	NaCl 2.0 M, surf. 1 %	N/C	5
B.subtilis 6051	Cu^{2+} $6.0 \cdot 10^{-2}$	AA $1.0 \cdot 10^{-1}$	1:5	NaCl 2.0 M, surf. 1 %	N/C	6 spores washed from PBS
B.subtilis 6051	Cu^{2+} $6.0 \cdot 10^{-2}$	AA $1.0 \cdot 10^{-1}$	1:5	surf. 1 %	N/C	7
B.subtilis 6051	Cu^{2+} $6.0 \cdot 10^{-2}$	AA $1.0 \cdot 10^{-1}$	1:5	-	N/C	8
B.subtilis 6051	Fe^{2+} $6.0 \cdot 10^{-2}$	AA $1.0 \cdot 10^{-1}$	1:5	-	N/C	9
B.subtilis 6051	Fe^{2+} $2.58 \cdot 10^{-4}$	H_2O_2 $1.5 \cdot 10^{-2}$	1:20	-	3	10

3.3 Results and discussion

In current study Fenton reaction was used to inactivate *B. subtilis* spores in water. Copper and iron were tested as catalysts for Fenton reaction. Hydrogen peroxide and ascorbic acid were tested as oxidants. Different ratios between oxidant and catalysts were also studied.

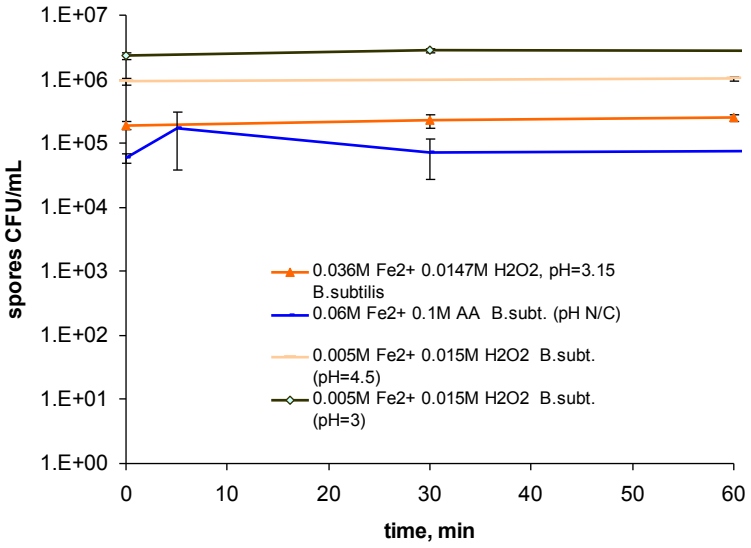

Figure 38: Inactivation of *B.subtilis* spores using iron as a transition metal for Fenton reaction

Treatment approach used by FEUP ($FeSO_4 \cdot 7H_2O$ $4.6 \cdot 10^{-4}$ mol + H_2O_2 $1.5 \cdot 10^{-2}$ mol; Run#1 and Run#10 in Table 2.1) for decomposition of paraquat (described in section 1) did not show significant reduction in concentration of viable (able to germinate) spores of *B. subtilis*. Probably the concentrations of active ingredients are too low to inactivate highly resistant spores (concentrations both of transit metal (Fe) ions and catalyst (H_2O_2) were the lowest among tested). It should be noted that none of the tested approaches using Fe as a catalyst resulted in visible spore reduction (see

Figure 38).

Probably amount of hydroxyl radicals formed in these reactions is not big enough to damage spore coat. Sagripanti (1992) showed that copper (used as a catalyst for Fenton reaction) is 5 times more active than iron. Thus copper was selected as a catalyst for the next set of experiments.

Treatment approach using Cu^{2+} $3.13 \cdot 10^{-2}$ mol and H_2O_2 $1.47 \cdot 10^{-2}$ mol inactivated 5-$\log_{10}$ *E.coli* cells within 5 minutes (concentration of viable *E.coli* cells did not change in control samples – at the same conditions but without hydrogen peroxide added) but had no such an effect on *B.subtilis* spores. This phenomenon can be explained by the fact that spores are much more resistant to the environmental stress and oxidants than vegetative cells.

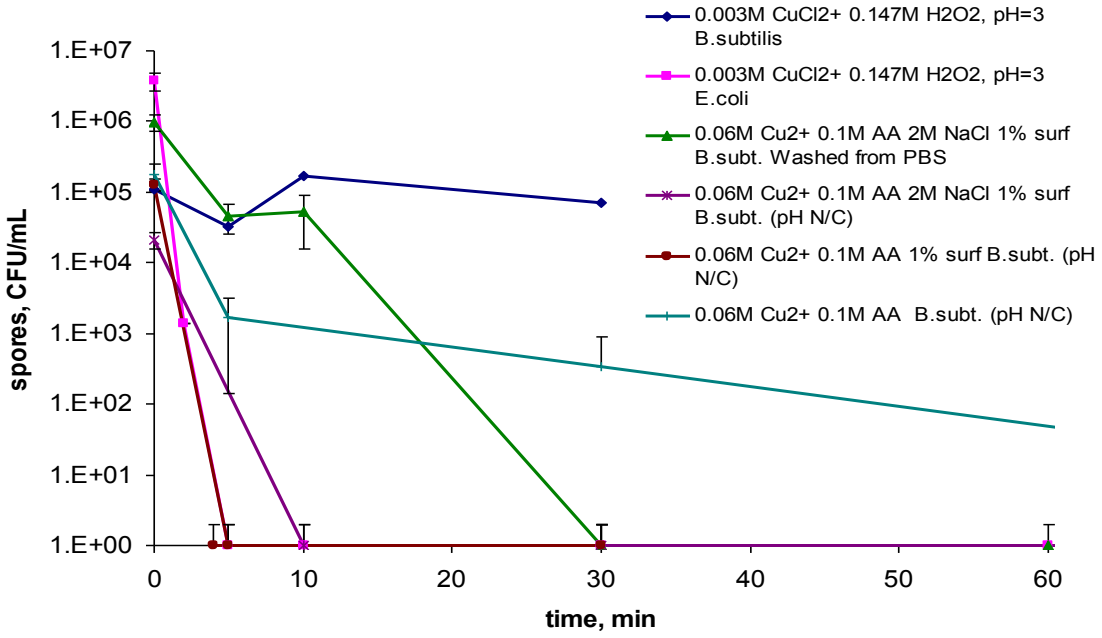

Figure 39: Inactivation of B.subtilis spores using copper as a transition metal for Fenton reaction

The best results in inactivation of *B.subtilis* spores were obtained using protocol suggested by Cross et al., (2003) (Cu^{2+} $6.0 \cdot 10^{-2}$, AA $1.0 \cdot 10^{-1}$ with addition of 2M NaCl and 1% of surfactant). This approach resulted in 5 $\log_{10}$ inactivation of *Bacillus* spores in 10 min. As mentioned in materials and methods *Bacillus* spore suspension was prepared in PBS buffer. If spores were washed from PBS, time necessary for inactivation increased from 10 min to 30 min (Figure 39). Obviously, salts presented in PBS benefit Fenton reaction which is in agreement with Cross et al., (2003). 5$\log_{10}$ *B.subtilis* spores were inactivated using just Cu and AA (without adding salt, surfactant, or pH correction) but the necessary time increased till 2 h. This result makes current treatment approach promising for using it in case of real contamination (no pH correction is needed).

pH values during reactions where iron was used as a catalyst were higher (see Figure 40 and Figure

41). It should be noted that pH values of all of the successful treatment approaches (for inactivation of *B.subtilis* spores) dropped below pH=2 shortly after beginning of the treatment. This phenomenon can be attributed to presence of AA in these experiments.

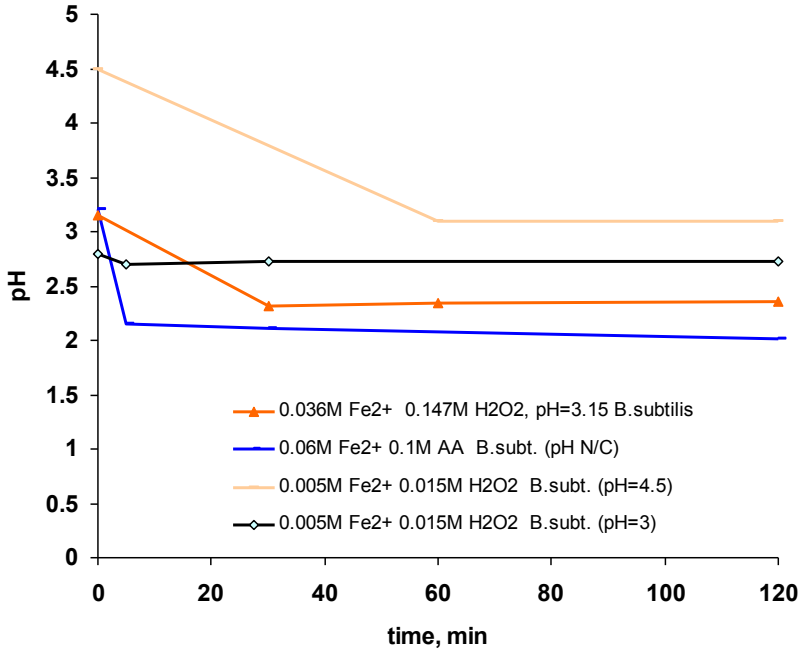

Figure 40: pH values during reactions where iron used as a transition metal

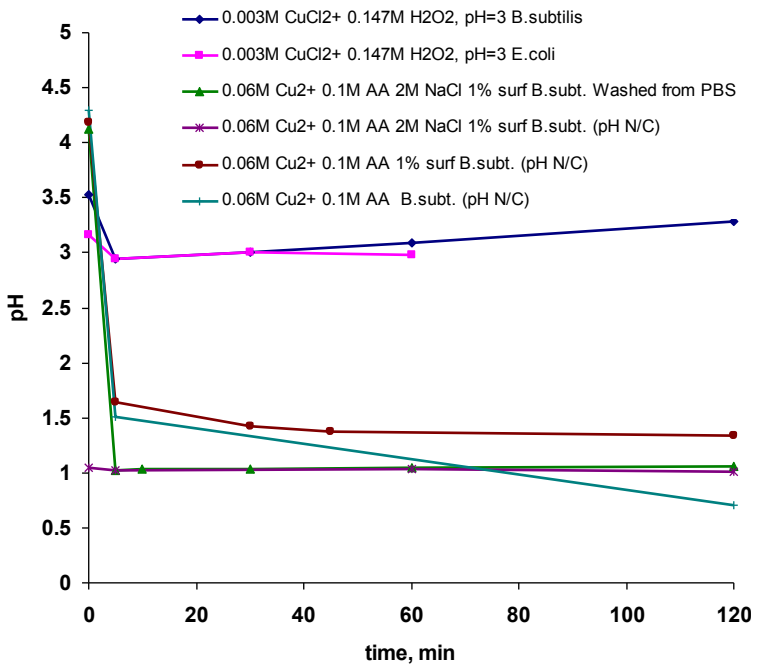

Figure 41: pH values during reactions where copper used as a transition metal

It is complicated to change the pH of water within the network and afterwards introduce the chemicals in real situation. No need in pH adjustment before Fenton reaction using copper as a catalyst is an advantage.

3.4 Conclusions

The results showed that it is possible to inactivate *B.subtilis* spores rapidly and effectively in water using Fenton reaction.

Effective inactivation of B.subtilis spores using copper as a transition metal and ascorbic acid as a catalyst can be achieved without pH correction.

Presence of salt and surfactant benefit Fenton reaction.

3.5 References

Bandala, E. R. (2009). Deactivation of Highly Resistant Microorganisms in Water Using Solar Driven Photocatalytic Processes Deactivation of Highly Resistant Microorganisms in Water Using Solar Driven Photocatalytic Processes. *International journal of chemical reactor engineering*, *7*.

Bandala Erick R., Pérez Roberto, Lee Angel Eduardo Velez, Sanchez-Salas Jose Luis, Quiroz Marco A., M.-R. M. A. (2011). Bacillus spore inactivation in water using photo assisted Fenton.pdf. *Sustainable environmental research*, *21*(5), 285-290.

Cross, J. B., Currier, R. P., Torraco, D. J., Vanderberg, L. A., Wagner, G. L., & Gladen, P. D. (2003). Killing of Bacillus Spores by Aqueous Dissolved Oxygen , Ascorbic Acid , and Copper Ions. *Applied and environmental microbiology*, *69*(4), 2245-2252.

Herbert, V. (1996). Prooxidant Effects of Antioxidant Vitamins. *The journal of nutrition*, *126*, 1197-1200.

Muranaka Hiroyuki, Suga Moritaka, Sato Keizo, Nakagawa Kazuko, Akaike Takaaki, Okamoto Tatsuya, Maeda Hiroshi, A. M. (1997). Superoxide scavenging activity of erythromycin–iron complex. *Biochemical and biophysical research communications*, *232*.

Neyens, E., & Baeyens, J. (2003). A review of classic Fenton's peroxidation as an advanced oxidation technique. *Journal of Hazardous Materials*, *98*(1-3), 33-50.

Niki, E. (1991). Action of ascorbic acid as a scavenger of active and stable oxygen radicals. *The American journal of clinical nutrition*, *54*(6 Suppl), 1119S-1124S.

Sagripanti, J. L. (1992). Metal-based formulations with high microbicidal activity. *Applied and environmental microbiology*, *58*(9), 3157-62.

Sagripanti, J. L., & Bonifacino, a. (1996). Comparative sporicidal effects of liquid chemical agents. *Applied and environmental microbiology*, *62*(2), 545-51.

Shapiro, M. P., Setlow, B., & Setlow, P. (2004). Killing of Bacillus subtilis Spores by a Modified Fenton Reagent Containing CuCl 2 and Ascorbic Acid. *Applied and environmenatal microbiology*, *70*(4), 2535-2539.